Figure 2 Core-dependent recruitment of active HCV replication complexes to the LD. (a) Huh-7 cells transfected with JFH1^{E2FL} RNA were analysed by *in situ* hybridization with strand-specific probes (plus or minus). The cells were labelled to simultaneously visualize lipid droplets (LDs), NS5A and Core (lower panels). Higher-magnification images of area 1 and area 2 are shown in the upper and middle right panels 1 and 2, respectively. Scale bars: 2 µm (panels 1, 2); 10 µm (lower right panel). (b) The percentages of JFH1^{E2FL}-, JFH1^{dC3}- and JFH1$^{PP/AA}$-expressing cells positive for overlapping signals for LDs and plus- or minus-strand hepatitis C virus (HCV) RNA (n > 200). (c) Intact or digitonin and nuclease-treated (dig/nuc) JFH1^{E2FL} replicon-bearing cells were analysed by *in situ* hybridization. The percentages of cells with overlapping signals for LD and plus- or minus-strand HCV RNA are shown (n > 200). (d) RNA-synthesizing activity in the LD fractions purified from cells transfected with JFH1^{E2FL}, JFH1^{dC3} or JFH1$^{PP/AA}$ RNA (top panel). As a control, HCV RNA synthesis activity in digitonin-permeabilized cells was analysed (second panel from the top). HCV protein levels represented by NS5A are shown, together with the level of tubulin (bottom two panels). (e) Localization of plus-strand HCV RNA and Core in JFH1^{dC3} replicon-bearing cells transfected with pcDNA3–Core^{Wt} (Scale bar, 10 µm). Uncropped images of gels are shown in Supplementary Information Fig. S6. All error bars are derived from s.d.

located in the perinuclear region (see Supplementary Information, Fig. S4a). More importantly, in about 20% of these cells, plus- and minus-strand RNAs accumulated around LDs (Fig. 2a, upper and middle panels; 2b) and colocalized with HCV proteins such as Core and NS5A (Fig. 2a, lower panels). No association between HCV RNA and LDs was detected in JFH1^{dC3}- or JFH1$^{PP/AA}$-replicating cells (Fig. 2b). Northern blot analysis revealed that 4.8% and 5.4% of total plus- and minus-strand HCV RNA, respectively, were detected in purified LD fractions of JFH^{E2FL}-replicating cells (data not shown). Induction of LD formation with oleic acid did not affect HCV RNA accumulation around LDs (data not shown). These results provide strong evidence that Core recruits HCV RNA as well as NS proteins to LDs.

The HCV replication complex is compartmentalized by lipid bilayer membranes[16–18]. Therefore, HCV RNA in the complex is resistant to nuclease treatment in digitonin-permeabilized cells[17] (Supplementary Information, Fig. S4b–d). *In situ* hybridization analysis did not reveal a significant difference in the number of cells containing LD-associated HCV RNA before and after nuclease treatment (Fig. 2c), indicating that HCV RNA around LDs is part of the replication complex. An RNA synthesis assay showed that the purified LD fraction from JFH1^{E2FL}-, but not JFH1^{dC3}- or JFH1$^{PP/AA}$-replicating cells, possessed HCV RNA synthesis activity, even though the expression levels of viral proteins and RNA-synthesizing activities in total cell lysates were similar (Fig. 2d). Moreover, the addition of Core^{Wt} rescued the localization of plus- and minus-strand
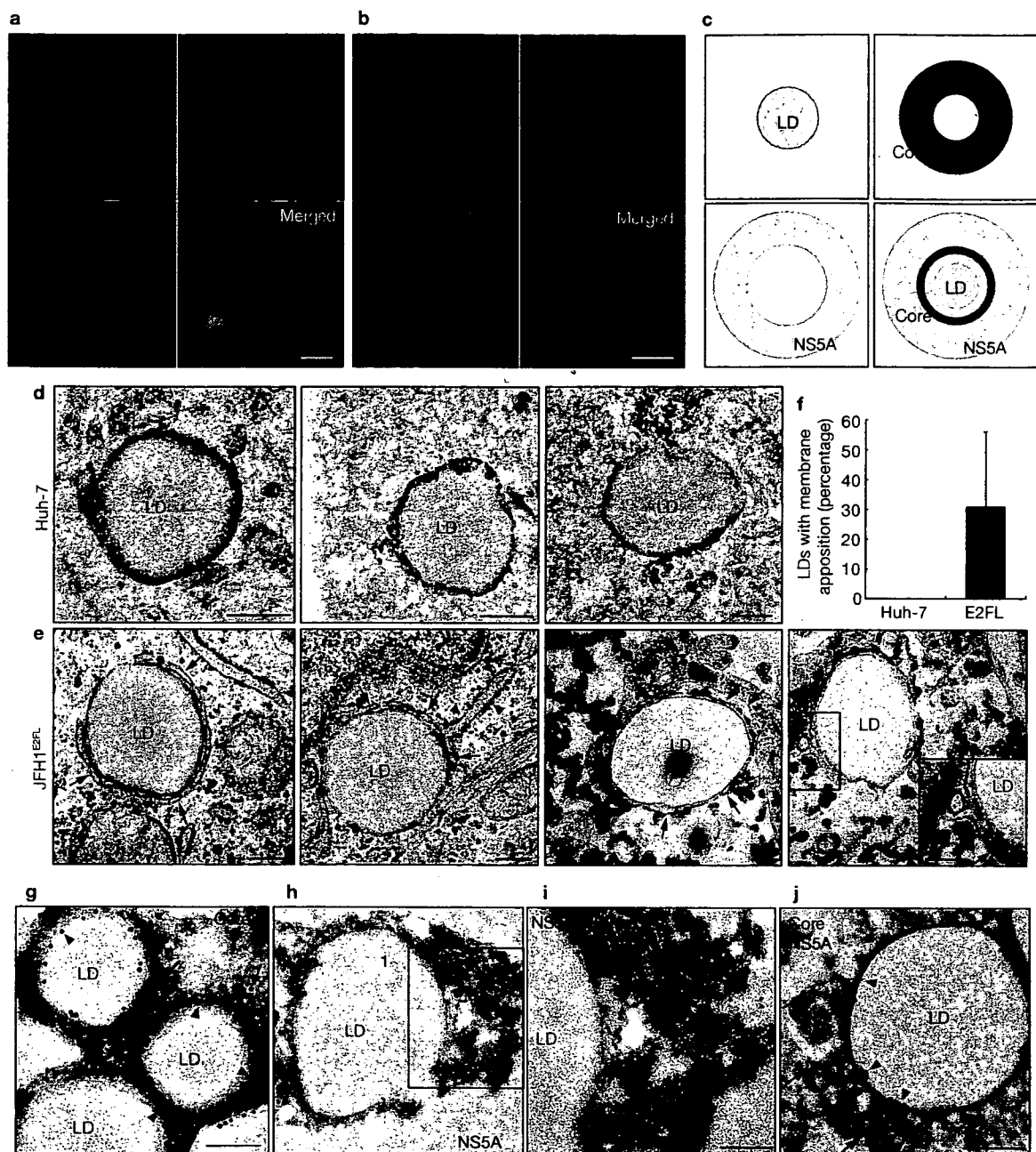
Figure 3 Spatial distribution of Core and NS5A relative to the LD.
(a, b) The localizations of Core, NS5A and ADRP around the lipid droplets (LDs) in JFH1^{E2FL} replicon-bearing cells were analysed using immunofluorescence microscopy. Scale bars, 1 μm. (c) Typical images of the localization of LDs, Core, NS5A and merged images are shown with the relative scale of each image. (d, e) Transmission electron micrographs of LDs in naïve Huh-7 cells and JFH1^{E2FL}-expressing cells. Arrows and arrowheads indicate LD-associated membranes and rough ER membranes, respectively. (f) Frequency of LDs with close appositions of membrane cisternae. About 100 Huh-7 cells or JFH1^{E2FL}-expressing cells, respectively, were chosen randomly. LDs with apposed membrane cisternae, as exemplified in panel e, were counted as positive. The LDs judged as positive were divided by the total number of LDs.
(g–j) Immunoelectron micrographs of LDs labelled with antibodies against Core (g), NS5A (h, i) or both (j) are shown. Panel i is a higher magnification of area 1 in panel h. In panel j, Core and NS5A are labelled with 15 nm and 10 nm gold particles, respectively. Scale bars, 200 nm. All error bars are derived from s.d.

HCV RNA around LDs in JFH^{dC3}-replicating cells (Fig. 2e and data not shown). Both plus- and minus-strand RNA associated with LDs were nuclease resistant (data not shown). These results demonstrate that Core recruits biologically active replication complexes to LDs.

The LD is surrounded by a phospholipid monolayer[19], whereas HCV replication complexes are likely to be surrounded by lipid bilayer membranes[16,17]. Therefore, the replication complexes might not be directly

associated with the membranes of LDs. To characterize the colocalization of LDs, viral proteins and replication complexes more precisely, we analysed the localization of NS5A with high-resolution immunofluorescence microscopy. Core was completely colocalized with ADRP, residing on the surface of LDs[20] (Fig. 3a), thus indicating that Core also directly associates with the surface of LDs. More importantly, NS5A mainly localized around the Core-positive area, resulting in a doughnut-shaped signal with a diameter slightly
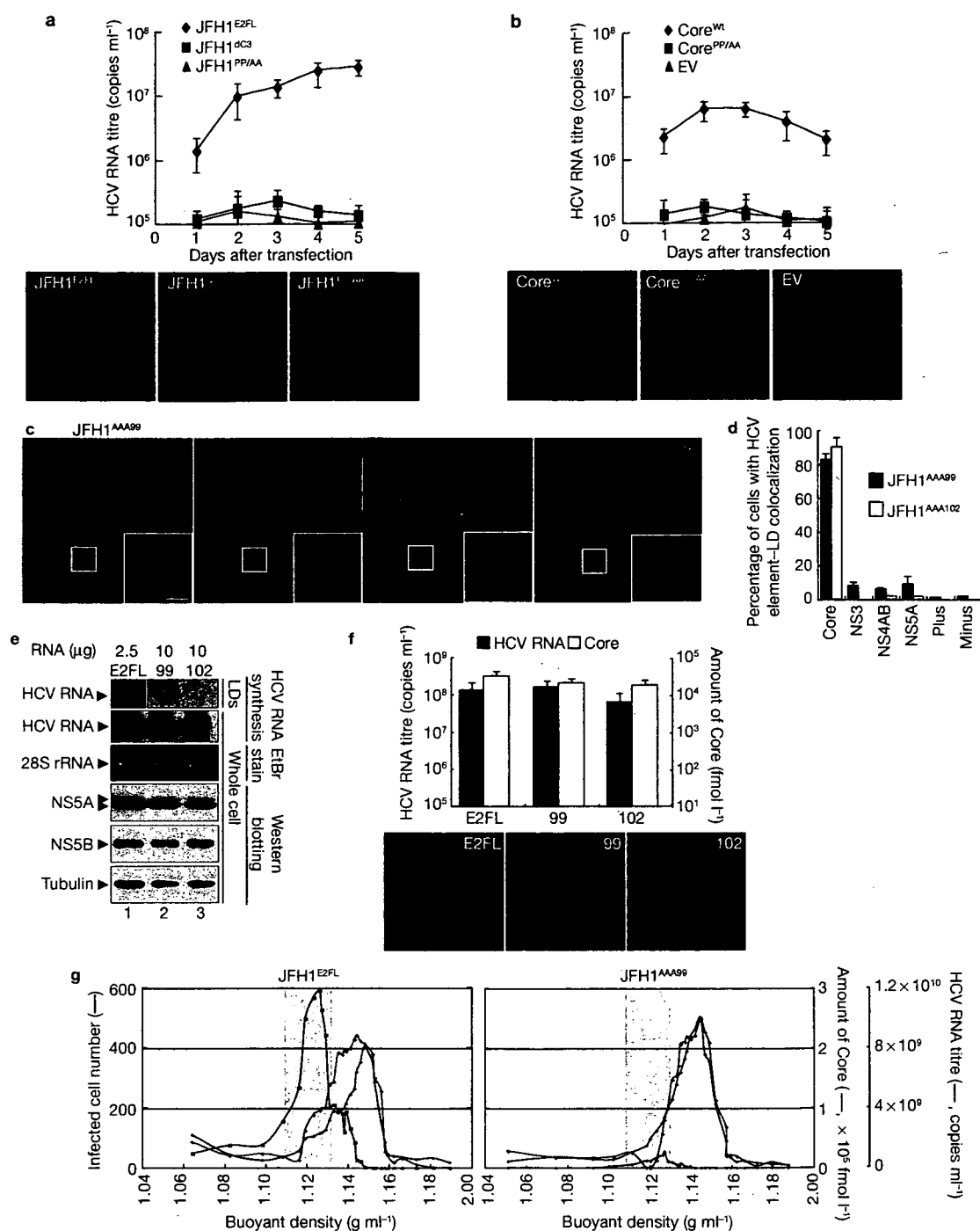
Figure 4 LD associations of Core and NS proteins are necessary for the production of infectious HCV particles. (a) The culture medium from JFH1^{E2FL}-, JFH1^{dC3}- or JFH1$^{PP/AA}$-replicating cells was collected at the indicated time points and the titre of hepatitis C virus (HCV) RNA was measured by real-time RT-PCR (upper panel, n = 3). The culture medium was added to naïve Huh7.5 cells and, 24 h after inoculation, and cells were labelled with anti-HCV antibodies (lower panels, red). (b) JFH1^{dC3} replicon-bearing cells were transfected with pcDNA3 (EV), pcDNA3-Core^{Wt} (Core^{Wt}) or pcDNA3-Core$^{PP/AA}$ (Core$^{PP/AA}$). The level of HCV RNA and the infectivity of the culture medium were examined as described above (n = 3). (c) Subcellular localization of NS5A and Core in cells expressing JFH1^{AAA99}. The insets are high magnifications of the area of the corresponding panel. Scale bar, 2 μm. (d) Percentages of cells in which the signals for given HCV proteins, and plus- and minus-strand HCV RNA, overlapped with those for LDs (n > 200). (e) Different amounts of JFH1^{E2FL} (E2FL), JFH1^{AAA99} (99) or JFH1^{AAA102} (102) RNAs, respectively, were transfected into the same number of

Huh-7 cells. HCV RNA synthesis activity in purified LD fractions (LD) and whole-cell lysates (whole cell) was analysed (HCV RNA synthesis). 28S rRNA was used as a control. Western blot analysis of NS5A, NS5B and tubulin in cells is also shown. All the RNA samples in the top panel were run on the same gel. (f) Analysis of HCV released from cells expressing JFH1^{E2FL}, JFH1^{AAA99} or JFH1^{AAA102}. HCV RNA titres (black bars) and amounts of Core (white bars) accumulated in the culture medium at 5 d after RNA transfection were measured (upper panel, n = 3). Infectivity of the culture medium for naïve Huh-7.5 cells was analysed as described above (lower panels). (g) Concentrated culture medium from JFH1^{E2FL}- and JFH1^{AAA99}-replicating cells was fractionated using 20–50% sucrose density-gradient centrifugation at 100,000 g for 16 h. For each fraction, the amounts of Core (black line), HCV RNA (blue line) and infectivity (represented by infected cell numbers in a well; red line) are plotted against the buoyant density (x-axis) (n = 3). Uncropped images of gels are shown in Supplementary Information Fig. S6. All error bars are derived from s.d.
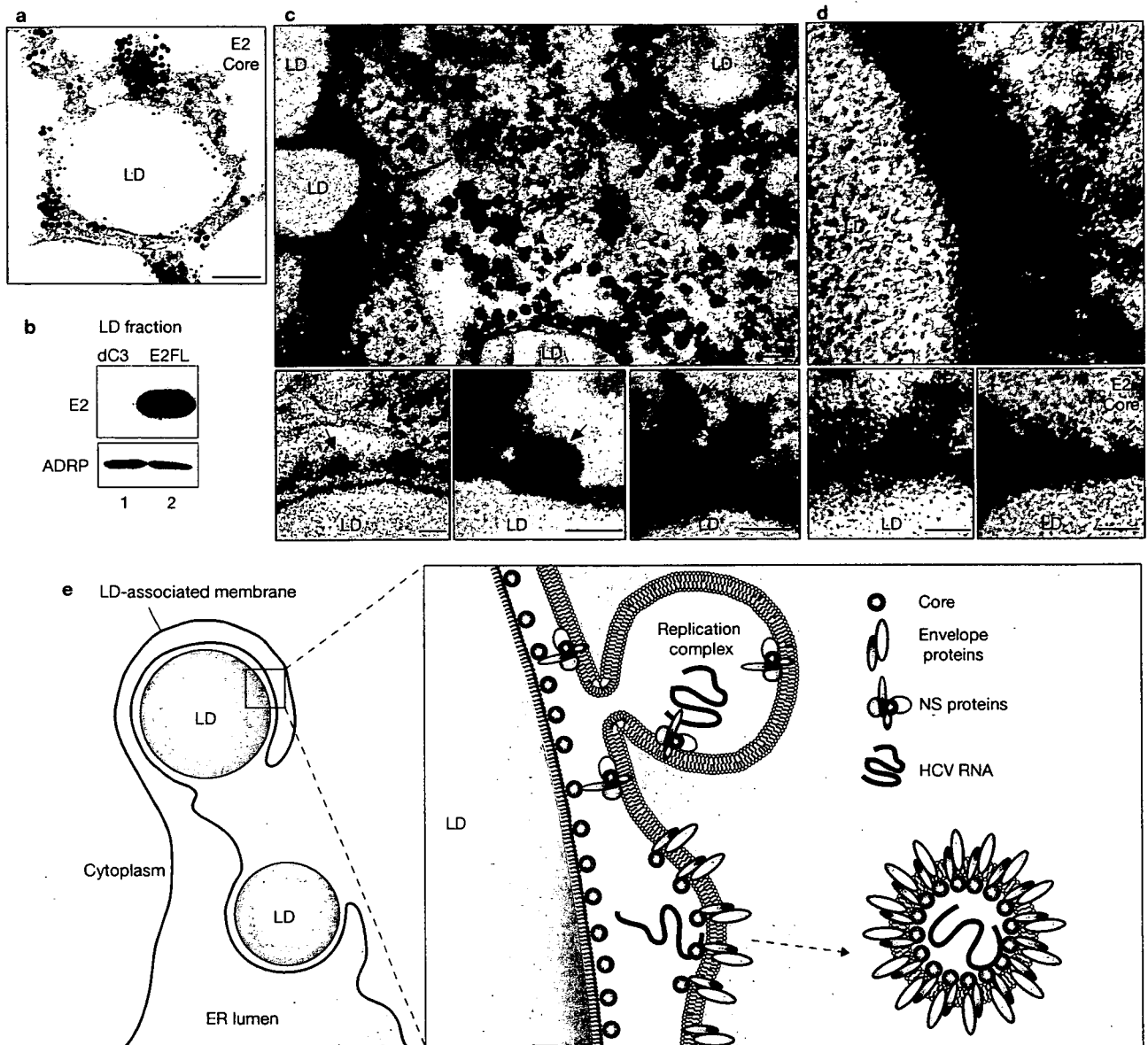
Figure 5 Virus-assembly takes place around the LDs. (a) Immunoelectron microscopic detection of E2 and Core in JFH1^{E2FL}-replicating cells. E2 and Core are labelled with 15 nm and 10 nm gold particles, respectively. (b) Western blot analysis of the lipid droplet (LD) fraction from JFH1^{E2FL} and JFH1^{dC3} replicon-bearing cells with anti-E2 and anti-ADRP antibodies. (c) Transmission electron micrographs of JFH1^{E2FL}-replicating cells. Arrows indicate virus-like particles. (d) Immunoelectron micrographs of LDs labelled with antibodies against Core (10 nm) and E2 (15 nm) are shown. Arrows show Core in electron-dense granules. Scale bar: a and upper panel of c: 100 nm; in d and lower panels of c: 50 nm. (e) A model for the production of infectious hepatitis C virus (HCV). Core mainly localizes on the monolayer membrane that surrounds the LD. HCV induces the apposition of the LD to the endoplasmic reticulum (ER)-derived bilayer membranes (LD-associated membrane). Core recruits NS proteins, as well as replication complexes, to the LD-associated membrane. NS proteins around the LD can then participate in infectious virus production. E2 also localizes around the LD. Through these associations, virion assembly proceeds in this local environment. Uncropped images of gels are shown in Supplementary Information Fig. S6.

larger than that of Core (Fig. 3b). The LD-proximal NS5A signal partially overlapped with the Core signal (Fig. 3b, c, grey). This concentric staining pattern was also observed with the other NS proteins (Supplementary Information, Fig. S5a), indicating that NS proteins associate with Core on the surface of LDs. Electron microscopic analysis only rarely revealed a close association of LDs with other organelles in naïve Huh-7 cells (Fig. 3d, f). However, in the case of JFH1^{E2FL}-replicating cells, about 30% of the LDs were in close proximity to membrane cisternae (Fig. 3e, arrows; 3f), arguing for a HCV-induced membrane rearrangement around LDs. Core was mainly located on the periphery of LDs, and occasionally signals were

observed in more distal areas of the LDs (Fig. 3g, arrowheads and arrows, respectively). Although some NS5A signals were observed on the surface of the LD, the majority of NS5A signals were detected more distal of LDs (Fig. 3h, i). Furthermore, we often observed membrane cisternae as white lines in the same area as NS5A signals (Fig. 3i, arrows). When the same section was labelled with anti-Core and anti-NS5A antibodies, Core was detected on the surface of the LDs, whereas NS5A was mainly observed in the peripheral area of the LDs (Fig. 3j, arrowheads and arrows, respectively). In summary, these results show that Core recruits NS proteins, as well as HCV replication complexes, to the LD-associated membranes.

The above results prompted us to ask whether Core–LD colocalization is important for the production of infectious virus particles. JFH1[E2FL]-replicating cells released virions into the culture medium and these viruses were highly infectious for naïve Huh-7.5 cells[11,21], although culture medium from JFH1[PP/AA]- or JFH1[dC3]-replicating cells did not contain significant levels of HCV RNA and infectious virus (Fig. 4a). However, following trans-complementation with Core[wt], a high titre of HCV RNA and infectious virus could be rescued from JFH1[dC3]-replicating cells (Fig. 4b; and see Supplementary Information, Fig. S5b, c). In contrast, the production of infectious viruses was not rescued by trans-complementation with Core[PP/AA] (Fig. 4b). RNA-binding properties and oligomerization of Core[wt] and Core[PP/AA], which are both necessary for virus assembly, were similar (Supplementary Information, Fig. S5d; ref. 22), arguing that the primary defect of this mutant in preventing infectious virus production is the inability to associate with LDs.

To investigate the contribution of NS proteins around LDs to infectious virus production, we used variants of NS5A, which were not recruited to LDs even in the presence of Core. We assumed that NS5A was crucial for recruiting other NS proteins to LDs, because the level of NS5A recruited to LDs via Core was higher than the levels of the other recruited NS proteins (Fig. 1c, JFH1[E2FL]). Using alanine-scanning mutagenesis within the NS5A coding region of JFH1[E2FL], we generated two mutants, JFH1[AAA99] and JFH1[AAA102], in which the amino-acid sequence APK (aa 99–101 of NS5A) or PPT (aa 102–104 of NS5A) was replaced by AAA (Supplementary Information, Fig. S1). In JFH1[AAA99]- and JFH1[AAA102]-replicating cells, NS5A was rarely detected around LDs, whereas Core was still localized to LDs (Fig. 4c, d). Importantly, these mutations impaired not only the NS5A association with LDs, but also the recruitment of other NS proteins and viral RNAs to LDs (Fig. 4d). These results indicate that NS5A is a key protein that recruits replication complexes to LDs. Importantly, HCV RNA synthesis activity in the LD fractions from these mutant JFH1-replicating cells was also severely impaired (Fig. 4e), corroborating the lack of association of HCV replication complexes with LDs.

To investigate the infectious virus production of these NS5A mutants, we prepared cells expressing similar levels of HCV proteins and RNA by adjusting the amount of transfected HCV RNA (Fig. 4e). This was necessary, because replication activities of these mutants were lower compared with JFH1[E2FL]. Under these conditions, the amounts of Core and HCV RNA that were released into the culture medium from cells transfected with the mutants were comparable to JFH[E2FL] (Fig. 4f, upper graph). However, infectivity titres of the mutants were severely reduced (Fig. 4f, lower panels). In sucrose density-gradient centrifugation of culture medium from JFH1[E2FL]-bearing cells, two types of HCV particles were detected: low-density particles (about 1.12 g ml^{−1}) with high infectivity (Fig. 4g, green area of JFH1[E2FL]), and high-density particles (about 1.15 g ml^{−1}) without infectivity (yellow area). This result indicates that only a minor portion of released HCV particles is infectious, whereas the majority of released particles lack infectivity. In contrast, cells bearing the JFH1[AAA99] mutant almost exclusively released non-infectious particles of around 1.15 g ml^{−1}, whereas infectious particles were barely detectable (Fig. 4g, JFH1[AAA99]). Taken together, these results provide convincing evidence that the association of NS proteins and replication complexes around LDs is critical for producing infectious viruses, whereas production of non-infectious viruses seems to follow a different pathway.

The results described so far imply that some step(s) of HCV assembly take place around LDs. To explore this possibility, we analysed the distribution of the major envelope protein E2 around the LD. Electron microscopic analysis revealed that, in about 90% of JFH1[E2FL]-replicating cells, E2 was localized in the peripheral area of the LDs (Fig. 5a, large grains). This labelling pattern was similar to the one observed for NS5A (Fig. 3j), indicating that E2 also localizes on the LD-associated membranes. Western blot analysis of the LD fraction supported this conclusion, because the LD fraction that was purified from JFH1[E2FL]-replicating cells, but not from JFH1[dC3]-replicating cells, contained E2 (Fig. 5b). Furthermore, spherical virus-like particles with an average diameter of about 50 nm were observed around LDs in JFH1[E2FL]-replicating cells (Fig. 5c, upper panel). These particles were never observed in naïve Huh-7 cells. A more refined analysis indicates that these particles are closely associated with membranes in close proximity to LDs (Fig. 5c, lower panels, arrows). Finally, these particles around the LDs reacted with Core- and E2-specific antibodies, arguing that the particles represent true HCV virions (Fig. 5d). These results suggest that infectious HCV particles are generated from the LD-associated membranous environment.

In this study, we have demonstrated that Core recruits NS proteins, HCV RNAs and the replication complex to LD-associated membranes. Mutations of Core and NS5A (Fig. 4), which failed to associate with LDs, impaired the production of infectious virus. We note that the mutant Core retains the ability to interact with RNA (Supplementary Information, Fig. S5b) and to assemble into nucleocapside[22]. Similarly, the NS5A mutant still supports viral genome replication and the formation of capsids or virus-like particles, arguing that the introduced mutations in Core and NS5A do not affect overall protein folding, stability or function (Fig. 4). Taken together, the data show that the association of HCV proteins with LDs is important for the production of infectious viral particles (Fig. 5e).

Our results also indicate that NS proteins around the LDs participate in the assembly of infectious virus particles. In one scenario, NS proteins may indirectly contribute to the different steps of virus production — for example, by establishing the microenvironment around the LDs that is required for infectious virus production. Alternatively, NS proteins around the LDs may directly participate in virus production — for example, as components of the replication complex that provide the RNA genome to the assembling nucleocapsid.

In support of the role of LDs in virus formation, we observed that colocalization of HCV protein with LDs was low in cases of the chimera Jc1, supporting up to 1,000-fold higher infectivity titres compared with JFH1 (ref. 13). In a Jc1-infected cell, only about 20% of LDs demonstrated detectable colocalization with Core, but this value increased to 80% in the case of a Jc1 mutant lacking most of the envelope glycoprotein genes and thus being unable to produce infectious virus particles (data not shown). This inverse correlation between the efficiency of virus production and Core protein accumulation on LDs indicates that rapid assembly and virus release results in the rapid liberation of HCV proteins from the LDs.

Steatosis and abnormal lipid metabolism caused by chronic HCV infection may be linked to enhanced LD formation[14]. In fact, the overproduction of LDs is induced by Core (Supplementary Information, Fig. S3) and HCV also induces membrane rearrangements around LDs (Fig. 3d–f). Our findings suggest that excessive Core-dependent formation of LDs

LETTERS

and membrane rearrangements are required to supply the necessary microenvironment for virus production. NS proteins and HCV RNA seem to be translocated from the ER to the LD-associated membranes. Interestingly, the LD-associated membranes were occasionally found in continuity with ribosome-studded rough ER (Fig. 3e, arrowheads). Thus, at least parts of the LD-associated membranes are likely to be derived from ER membranes. ER marker proteins, however, were not detected in the LD fraction, suggesting that the LD-associated membrane is characteristically distinct from that of ER membranes.

To our knowledge, this is the first report showing that LDs are required for the formation of infectious virus particles. The fact that capsid protein of the hepatitis G virus also localizes to LDs[15] indicates that LDs might be important for the production of other viruses as well. Our findings demonstrate a novel function of LDs, provide an important step towards elucidating the mechanism of HCV virion production and open new avenues for novel antiviral intervention. □

METHODS

Antibodies. The antibodies used for immunoblotting and immunolabelling were specific for Core (#32-1 and RR8); E2 (AP-33 (ref. 23); 3/11, CBH5 and Flag M2 (Sigma-Aldrich, St Louis, MO); NS3 (R212)[17]; NS4A and 4B (PR12); NS5A (NS5ACL1); NS5B (NS5B-6 and JFH1-1)[24]; ADRP (Progen Biotechnik, Heidelberg, Germany); tubulin (Oncogene Research Products, MA, USA); Grp78 (StressGen, Victoria, Canada); PDI (StressGen); and Calnexin-NT (StressGen). Antibodies specific for Core (#32-1 and RR8), NS3 (R212) and NS4AB (PR12) were gifts from Dr Kohara (The Tokyo Metropolitan Institute of Medical Science, Japan). Anti-E2 antibody (AP-33) was provided by Dr Patel (MRC Virology Unit, UK). Anti-NS5B (NS5B-6) antibody was kindly provided by Dr Fukuya (Osaka University, Japan). Rabbit polyclonal antibodies specific for NS5A were raised against a bacterially expressed GST-NS5A (1–406 aa) fusion protein. In the case of the HCV chimeras Con1/C3 and H77/C3, immunofluorescence analyses were performed by using the following antibodies: Core (C7/50)[5], a JFH1 NS3-specific rabbit polyclonal antiserum; NS4B (#86)[25]; and NS5A (Austral Biologicals, San Ramon, CA).

Indirect immunofluorescence analysis. Indirect immunofluorescence analysis was performed essentially as described previously[17], with slight modifications. Cells transfected with JFH1 RNA were seeded onto a collagen-coated Labtech II 8-well chamber (Nunc, NY, USA). The coating with collagen was performed using rat-tail collagen type I (BD Bioscience, Palo Alto, CA) according to manufacturer's instructions. Three days after seeding, the cells were washed twice with phosphate-buffered saline (PBS; 137 mM NaCl, 2.7 mM KCl, 4.3 mM Na$_2$HPO$_4$ and 1.4 mM KH$_2$PO$_4$) and fixed with fixation solution (4% paraformaldehyde and 0.15 M sodium cacodylate at pH 7.4) for 15 min at room temperature. After washing with PBS, the cells were permeabilized with 0.05% Triton X-100 in PBS for 15 min at room temperature. For the precise localization of the proteins, the cells were permeabilized with 50 μg ml^{-1} of digitonin in PBS for 5 min at room temperature[26]. After incubating the cells with blocking solution (10% fetal bovine serum and 5% bovine serum albumin (BSA) in PBS) for 30 min, the cells were incubated with the primary antibodies. The fluorescent secondary antibodies were Alexa 568- or Alexa 647-conjugated anti-mouse or anti-rabbit IgG antibodies (Invitrogen, Carlsbad, CA). Nuclei were labelled with 4′,6-diamidino-2-phenylindole (DAPI). LDs were visualized with BODIPY 493/503 (Invitrogen). Analyses of JFH1 were performed on a Leica SP2 confocal microscope (Leica, Heidelberg, Germany). Analysis of the Con1/C3 and the H77/C3 chimeras was performed in the same way, except that imaging was performed on a Nikon C1 confocal microscope (Nikon, Tokyo, Japan).

Electron microscopy. For conventional electron microscopy, cells cultured in plastic Petri dishes were processed *in situ*. The cells were fixed in 2.5% glutaraldehyde and 0.1 M sodium phosphate (pH 7.4), and then in OsO$_4$ and 0.1 M sodium phosphate (pH 7.4). The cells were then dehydrated in a graded ethanol series and embedded in an epoxy resin. Ultrathin sections were cut perpendicular to the base of the dish. For immuno-electron microscopy, cells were detached

from the dish with a cell scraper after fixation in 4% paraformaldehyde, 0.1% glutaraldehyde and 0.1 M sodium phosphate (pH 7.4) for 24 h, and washed in 0.1 M lysine, 0.1 M sodium phosphate (pH 7.4) and 0.15 M sodium chloride. After dehydrating the cells in a graded series of cold ethanol, they were embedded in Lowicryl K4M at –20 °C. Ultrathin sections were labelled with primary antibodies and colloidal gold particles (15 nm) conjugated to anti-mouse IgG or anti-rabbit IgG antibodies. For double labelling, colloidal gold particles with different diameters (10 nm and 15 nm) conjugated to anti-mouse IgG or anti-rabbit antibodies were used. Samples were observed after staining with uranyl acetate and lead citrate with a JEM 1010 electron microscope at the accelerating voltage of 80 kV. Anti-Core (#32-1 and RR88), anti-NS5A (NS5ACL1) and anti-E2 (Flag M2) antibodies were used.

Preparation of the lipid droplets. Cells at a confluency of ~80% on a dish with a diameter of 14 cm were scraped in PBS. The cells were pelleted by centrifugation at 1,500 rpm. The pellet was resuspended in 500 μl of hypotonic buffer (50 mM HEPES, 1 mM EDTA and 2 mM MgCl$_2$ at pH 7.4) supplemented with protease inhibitors (Roche Diagnostics, Basel, Switzerland) and was incubated for 10 min at 4 °C. The suspension was homogenized with 30 strokes of a glass Dounce homogenizer using a tight-fitting pestle. Then, 50 μl of 10× sucrose buffer (0.2 M HEPES, 1.2 M KoAc, 40 mM Mg(oAc)$_2$ and 50 mM DTT at pH 7.4) was added to the homogenate. The nuclei were removed by centrifugation at 2,000 rpm for 10 min at 4 °C. The supernatant was collected and centrifuged at 16,000 g for 10 min at 4 °C. The supernatant (S16) was mixed with an equal volume of 1.04 M sucrose in isotonic buffer (50 mM HEPES, 100 mM KCl, 2 mM MgCl$_2$ and protease inhibitors). The solution was set at the bottom of 2.2-ml ultracentrifuge tube (Hitachi Koki, Tokyo, Japan). One milliliter of isotonic buffer was loaded onto the sucrose mixture. The tube was centrifuged at 100,000 g in an S55S rotor (Hitachi Koki) for 30 min at 4 °C. After the centrifugation, the LD fraction on the top of the gradient solution was recovered in isotonic buffer. The suspension was mixed with 1.04 M sucrose and centrifuged again at 100,000 g, as described above, to eliminate possible contamination with other organelles. The collected LD fraction was used for western blotting or the HCV RNA synthesis assay.

HCV RNA synthesis assay. An assay of HCV RNA synthesis using digitonin-permeabilized cells was performed as described previously[17]. For RNA synthesis assays using the LD fraction, the LD fraction collected by sucrose-gradient sedimentation was suspended in buffer B, which contained 2 mM manganese (II) chloride, 1 mg ml^{-1} acetylated BSA (Nacalai Tesque, Kyoto, Japan), 5 mM phosphocreatine (Sigma), 20 units/ml creatine phosphokinase (Sigma), 50 μg ml^{-1} actinomycin D, 500 μM ATP, 500 μM CTP, 500 μM GTP (Roche Diagnostics) and 1.85 MBq of [α-^{32}P] UTP (GE Healthcare, Little Chalfont, UK), and incubated at 27 °C for 4 h. The reaction products were analysed by gel electrophoresis followed by autoradiography.

Note: Supplementary Information is available on the Nature Cell Biology website.

AUTHOR CONTRIBUTIONS
Y.M. and K.S. planned experiments and analyses. Y.M. was responsible for experiments for Figs 1, 2, 3a–c, 4a–e and 5b. K.A., N.U., electron microscopy; T.H., Fig. 1e; M.Z., R.B., Fig. S2e; and K.S. and K.W., Fig. 4f–g. T.W. provided JFH1 strain. Y.M. and K.S. wrote the manuscript. All authors discussed the results and commented on the manuscript.

1. Martin, S. & Parton, R. G. Lipid droplets: a unified view of a dynamic organelle. *Nature Rev. Mol. Cell Biol.* **7**, 373–378 (2006).
2. Blanchette-Mackie, E. J. *et al.* Perilipin is located on the surface layer of intracellular lipid droplets in adipocytes. *J. Lipid Res.* **36**, 1211–1226 (1995).
3. Vock, R. *et al.* Design of the oxygen and substrate pathways. VI. structural basis of intracellular substrate supply to mitochondria in muscle cells. *J. Exp. Biol.* **199**, 1689–1697 (1996).
4. Liang, T. J. *et al.* Viral pathogenesis of hepatocellular carcinoma in the United States. *Hepatology* **18**, 1326–1333 (1993).
5. Moradpour, D., Englert, C., Wakita, T. & Wands, J. R. Characterization of cell lines allowing tightly regulated expression of hepatitis C virus core protein. *Virology* **222**, 51–63 (1996).
6. Deleersnyder, V. *et al.* Formation of native hepatitis C virus glycoprotein complexes. *J. Virol.* **71**, 697–704 (1997).
7. Kato, N. *et al.* Molecular cloning of the human hepatitis C virus genome from Japanese patients with non-A, non-B hepatitis. *Proc. Natl Acad. Sci. USA* **87**, 9524–9528 (1990).
8. Hijikata, M. & Shimotohno, K. [Mechanisms of hepatitis C viral polyprotein processing]. *Uirusu* **43**, 293–298 (1993).
9. Dubuisson, J., Penin, F. & Moradpour, D. Interaction of hepatitis C virus proteins with host cell membranes and lipids. *Trends Cell Biol.* **12**, 517–523 (2002).
10. Wakita, T. *et al.* Production of infectious hepatitis C virus in tissue culture from a cloned viral genome. *Nature Med.* **11**, 791–796 (2005).
11. Lindenbach, B. D. *et al.* Complete replication of hepatitis C virus in cell culture. *Science* **309**, 623–626 (2005).
12. Zhong, J. *et al.* Robust hepatitis C virus infection in vitro. *Proc. Natl Acad. Sci. USA* **102**, 9294–9299 (2005).
13. Pietschmann, T. *et al.* Construction and characterization of infectious intragenotypic and intergenotypic hepatitis C virus chimeras. *Proc. Natl Acad. Sci. USA* **103**, 7408–7413 (2006).
14. Moriya, K. *et al.* Hepatitis C virus core protein induces hepatic steatosis in transgenic mice. *J. Gen. Virol.* **78**, 1527–1531 (1997).
15. Hope, R. G., Murphy, D. J. & McLauchlan, J. The domains required to direct core proteins of hepatitis C virus and GB virus-B to lipid droplets share common features with plant oleosin proteins. *J. Biol. Chem.* **277**, 4261–4270 (2002).
16. Egger, D. *et al.* Expression of hepatitis C virus proteins induces distinct membrane alterations including a candidate viral replication complex. *J. Virol.* **76**, 5974–5984 (2002).
17. Miyanari, Y. *et al.* Hepatitis C virus non-structural proteins in the probable membranous compartment function in viral genome replication. *J. Biol. Chem.* **278**, 50301–50308 (2003).
18. Quinkert, D., Bartenschlager, R. & Lohmann, V. Quantitative analysis of the hepatitis C virus replication complex. *J. Virol.* **79**, 13594–13605 (2005).
19. Tauchi-Sato, K., Ozeki, S., Houjou, T., Taguchi, R. & Fujimoto, T. The surface of lipid droplets is a phospholipid monolayer with a unique fatty acid composition. *J. Biol. Chem.* **277**, 44507–44512 (2002).
20. Londos, C., Brasaemle, D. L., Schultz, C. J., Segrest, J. P. & Kimmel, A. R. Perilipins, ADRP, and other proteins that associate with intracellular neutral lipid droplets in animal cells. *Semin. Cell Dev. Biol.* **10**, 51–58 (1999).
21. Blight, K. J., McKeating, J. A. & Rice, C. M. Highly permissive cell lines for subgenomic and genomic hepatitis C virus RNA replication. *J. Virol.* **76**, 13001–13014 (2002).
22. Klein, K. C., Dellos, S. R. & Lingappa, J. R. Identification of residues in the hepatitis C virus core protein that are critical for capsid assembly in a cell-free system. *J. Virol.* **79**, 6814–6826 (2005).
23. Owsianka, A. *et al.* Monoclonal antibody AP33 defines a broadly neutralizing epitope on the hepatitis C virus E2 envelope glycoprotein. *J. Virol* **79**, 11095–11104 (2005).
24. Ishii, N. *et al.* Diverse effects of cyclosporine on hepatitis C virus strain replication. *J. Virol.* **80**, 4510–4520 (2006).
25. Lohmann, V., Korner, F., Herian, U. & Bartenschlager, R. Biochemical properties of hepatitis C virus NS5B RNA-dependent RNA polymerase and identification of amino acid sequence motifs essential for enzymatic activity. *J. Virol* **71**, 8416–8428 (1997).
26. Ohsaki, Y., Maeda, T. & Fujimoto, T. Fixation and permeabilization protocol is critical for the immunolabeling of lipid droplet proteins. *Histochem. Cell Biol.* **124**, 445–452 (2005).

To order reprints, please contact:

In the Americas:
Tel +1 212 726 9631; Fax 212 679 0843; reprints@natureny.com

Europe/UK/ROW:
Tel +44 (0)20 7843 4967; Fax + 44 (0)20 7843 4839; reprints@nature.com

Japan & Korea:
Tel +81 3 3267 8751; Fax +81 3 3267 8746; reprints@naturejpn.com

Anti-hepatitis C Virus Activity of Tamoxifen Reveals the Functional Association of Estrogen Receptor with Viral RNA Polymerase NS5B*

Koichi Watashi, Daisuke Inoue, Makoto Hijikata, Kaku Goto, Hussein H. Aly, and Kunitada Shimotohno[1]

From the Department of Viral Oncology, Institute for Virus Research, Kyoto University, 53 Kawaharacho, Shogoin, Sakyo-ku, Kyoto 606-8507, Japan

Hepatitis C virus (HCV) is a major causative agent of hepatocellular carcinoma. HCV genome replication occurs in the replication complex (RC) around the endoplasmic reticulum membrane. However, the mechanisms regulating the HCV RC remain widely unknown. Here, we used a chemical biology approach to show that estrogen receptor (ESR) is functionally associated with HCV replication. We found that tamoxifen suppressed HCV genome replication. Part of ESRα resided on the endoplasmic reticulum membranes and interacted with HCV RNA polymerase NS5B. RNA interference-mediated knockdown of endogenous ESRα reduced HCV replication. Mechanistic analysis suggested that ESRα promoted NS5B association with the RC and that tamoxifen abrogated NS5B-RC association. Thus, ESRα regulated the presence of NS5B in the RC and stimulated HCV replication. Moreover, the ability of ESRα to regulate NS5B was suggested to serve as a potential novel target for anti-HCV therapeutics.

Estrogen receptor (ESR)[2] belongs to the steroid hormone receptor family of the nuclear receptor superfamily (1). ESR consists of two subtypes, ESRα and ESRβ. As a primary physiological function, ESR is involved in the transcription for downstream genes in response to stimulation by the ligand, estradiol. In the normal state, ESR is mainly located in the cytoplasm and nucleus. Upon binding of the ligand, ESR dimerizes and translocates into the nucleus, where it binds to the ESR-responsive

elements (ERE) in the DNA promoter of downstream genes and drives transcription. In addition to this classical genomic action, a portion of ESR is located on the membrane, such as the plasma membrane, and involved in the nongenomic function of triggering signal transduction pathways, such as mitogen-activated protein kinase, phosphatidylinositol 3-kinase, and protein kinase C (2–4). Although the molecular basis of ESR membrane retention is not fully understood, one mechanism involves a membrane protein, caveolin (CAV); ESRα interacted with CAV, and this interaction facilitated ESRα localization to the membrane (5, 6). It was also reported that ESRα localizes to the lipid rafts on the plasma membrane (7). The lipid rafts are microdomains of the membrane that form platforms enriched in cholesterol and glycosphingolipids. However, the characteristics and relevance of membrane-associated ESR have not been fully disclosed. Here, we report the novel role of ESRα in the regulation of viral replication.

Hepatitis C virus (HCV), a causative agent of chronic hepatitis, liver cirrhosis, and hepatocellular carcinoma, constitutes a serious health problem worldwide (8). HCV has a positive strand RNA genome that produces at least 10 functional viral proteins: core, envelope 1, envelope 2, p7, nonstructural protein 2 (NS2), NS3, NS4A, NS4B, NS5A, and NS5B (9, 10). NS5B is an RNA-dependent RNA polymerase, which plays a central role in viral genome replication (11, 12). HCV genome replication can be evaluated using a HCV subgenomic replicon system, which Lohmann *et al.* (13) first established. In this system, cells carry an HCV subgenome RNA encoding NS3 to NS5B. Using this system, it has been proposed that HCV genome replication occurs in the replication complex (RC), which contains the viral genome RNA and HCV NS proteins. The RC forms on the surface of the intracellular membranes, including the endoplasmic reticulum (ER) membrane, and is surrounded by a membrane structure (14–17). It also has been reported that HCV genome replication associates with the lipid rafts on these intracellular membranes, such as the ER membrane (14, 18). These lipid rafts accumulate CAV2, and HCV proteins involved in viral genome replication cofractionate with CAV2 (18). However, it is largely unknown how the RC is formed and under what mechanism the HCV proteins participate in the RC.

A chemical biology approach is a useful method to analyze the molecular mechanism of viral life cycles as well as cellular physiological processes (19). We employed forward chemical genetics in which we analyzed HCV replication activity as a phenotypic indicator of a cell-based assay to screen chemical

[1] To whom correspondence should be addressed: Dept. of Viral Oncology, Institute for Virus Research, Kyoto University, 53 Kawaharacho, Shogoin, Sakyo-ku, Kyoto 606-8507, Japan. Tel.: 81-75-751-4000; Fax: 81-75-751-3998; E-mail: kshimoto@virus.kyoto-u.ac.jp.
[2] The abbreviations used are: ESR, estrogen receptor; HCV, hepatitis C virus; RC, replication complex; ER, endoplasmic reticulum; TAM, tamoxifen; ERE, ESR-responsive element(s); CAV, caveolin; NS, nonstructural protein; MM, microsomal membrane; siRNA, small interfering RNA; si-ESR, small interfering ESR; GST, glutathione S-transferase; aa, amino acid(s); RT, reverse transcription; NS3, NS4A, NS4B, NS5A, and NS5B, nonstructural protein 3, 4A, 4B, 5A, and 5B, respectively.

compounds that inhibited HCV replication. Using this system, we previously identified an immunosuppressant, cyclosporin A, as an anti-HCV compound (20). We also reported that cyclophilin B regulated the RNA binding activity of NS5B (21). In the current study, this chemical screening approach linked ESRα to HCV replication. We showed that tamoxifen (TAM) suppressed HCV genome replication. Using TAM as a bioprobe, we found that ESRα interacted with NS5B and regulated the participation of NS5B in the RC.

EXPERIMENTAL PROCEDURES

Cell Culture and Transfection—Huh-7 and cured MH-14 cells (21) were cultured in Dulbecco's modified Eagle's medium (Invitrogen) supplemented with 10% fetal bovine serum, minimal essential medium nonessential amino acid (Invitrogen), and kanamycin (Meiji). MH-14 cells, carrying HCV subgenomic replicon (16), and LucNeo#2 cells, carrying luciferase-containing subgenomic replicon (22), were cultured in the same medium supplemented with 300 µg/ml G418 (Invitrogen). Hus-E7/DN24 cells, a human hepatocyte cell line established by immortalization with HPV E6E7 and hTERT from human primary hepatocytes and introduction with a dominant negative form of interferon regulatory factor-7 (23), were cultured with Dulbecco's modified Eagle's medium with 20 mM Hepes (Invitrogen), 15 g/ml L-proline, 0.25 g/ml insulin (Sigma), 50 nM dexamethasone (Sigma), 44 mM NaHCO$_3$, 10 mM nicotinamide, 5 ng/ml epidermal growth factor, 0.1 mM Asc-2P, 100 IU/ml penicillin G (Invitrogen), 100 µg/ml streptomycin (Invitrogen), 5% fetal bovine serum, 1% Dulbecco's modified Eagle's medium, and 2 UG/ml Fungizone (Invitrogen) (24). Plasmid transfection was performed with FuGENE 6 transfection reagent (Roche Applied Science), as described previously (25). RNA transfection was achieved using DMrie-C transfection reagent (Invitrogen), as described previously (21). siRNA was transfected by using siLentFect (Bio-Rad) (21).

Plasmid Construction—pCMV-FL-ESRα, encoding the whole open reading frame of ESRα fused with a FLAG tag, was generated by inserting the PCR product using 5'-GTTGAAT-TCATGACCATGACCCTCCAC-3' and 5'-GTTGATCTCG-AGTCAGACTGTGGCAGGGAAAC-3' as primer set and human lymphocyte cDNA library (Clontech) as a template into the EcoRI-XhoI site of pCMV-FLAG vector (21). pCAG-HA-NS5B, encoding the NS5B protein fused with a hemagglutinin tag, was made by subcloning the PCR product with 5'-GTTG-CGGCCGCTATGTCAATGTCCTACTCA-3' and 5'-GTTC-TCGAGTCACCGGTTGGGGAGCAGGTA-3' as primers and pMH14 as a template into NotI-XhoI digestion of PCAG-HA vector (21). Expression plasmids for HCV NS3, NS4B, NS5A, and NS5B (pcDNA-NS3, pcDNA-NS4B, pcDNA-NS5A, and pcDNA-NS5B, respectively) were described in Ref. 21. pGEX-ESRα A/B, C, D, and E/F, expressing the fusion protein of the domain A/B, C, D, and E/F of ESRα with GST, were prepared by the insertion of the PCR product with pCMV-FL-ESRα as a template and appropriate primers into the EcoRI-XhoI site of pGEX-6P1 vector (Clontech). The expression plasmids for the point mutants of ESRα, ESRα(L540Q), ESRα(255M), and ESRα(258M), of which Leu at aa 540, IRK at aa 255–257, and DRR at aa 258–260 were replaced by Gln, TGT, and ANT, respec-

tively, was generated by oligonucleotide-directed mutagenesis. pCMV-FL-CAV2, encoding FLAG-tagged CAV2, was prepared by inserting the PCR product amplified with 5'-GTTGTCGACT-ATGGGGCTGGAGAC-3' and 5'-GTTAAGCTTTCAATCCT-GGCTC-3' as primers and human liver cDNA library (Clontech) as a template into the SalI-HindIII site of pCMV-FLAG vector (21). The mammalian expression vector for the C domain of ESRα was generated by replacing the EcoRI-XhoI digestion of pCMV-FLAG vector (21) by that of pGEX-ESRα C. pLMH14 was described previously (26). pGL3-EREX3-TATA-Luc, pcDNA3-ERα, pcDNA3-hERβ were kindly provided by Dr. Kato (Institute of Molecular and Cellular Biosciences, University of Tokyo). JFH1 expression plasmid was provided by Dr. Wakita (National Institute of Infectious Diseases).

Luciferase Assay—A luciferase assay monitoring HCV replication activity was performed as described previously (22, 26). In Fig. 1, *A* and *F*, we used LucNeo#2 cells, stably carrying luciferase-containing subgenomic replicon (22). In Figs. 2 (*D* and *E*), 4C, and 6A, we transiently transduced luciferase-containing replicon LMH14 RNA together with each expression plasmid into cured MH-14 cells (26). A luciferase assay detecting the transcriptional activity driven from the ERE was performed as described previously (25).

Real Time RT-PCR Analysis—Real time RT-PCR analysis was performed as previously described (20).

Immunoblot Analysis—Immunoblot analysis was performed as previously described (25). The antibodies used in this study are anti-NS5A (kindly provided by Dr. Takamizawa (Osaka University)), anti-NS5B (anti-NS5B#14; a generous gift from Dr. Kohara (Tokyo Metropolitan Institute of Medical Science)), anti-NS5B (NS5B#6; a kind gift from Dr. Fukuya (Osaka University)), anti-tubulin (Oncogene), anti-FLAG (Sigma), anti-IκBα (Santa Cruz Biotechnology, Inc., Santa Cruz, CA), anti-calnexin (StressGen), and anti-caveolin-2 antibodies (BD Biosciences Pharmingen).

Indirect Immunofluorescence Analysis—Indirect immunofluorescence analysis was performed as described previously (25). The antibodies used were anti-NS5A and anti-protein-disulfide isomerase antibodies (StressGen).

siRNA—siRNA duplexes (5'-GUGUGCAAUGACUAUGC-UUCA-3' for si-ESRα and 5'-CGCAUCGGGAUAUCACUA-UGG-3' for si-ESRβ) were synthesized (Proligo). A randomized siRNA, si-control, was purchased from Dharmacon (nonspecific control duplex IX).

Enzyme-linked Immunosorbent Assay—HCV core was quantified in the culture medium of the cells transfected with JFH1 RNA (29) with an enzyme-linked immunosorbent assay according to the manufacturer's protocol (HCV antigen enzyme-linked immunosorbent assay test; Ortho-Clinical Diagnostics).

RT-PCR Analysis—RT-PCR analysis was performed as described (20) by using the following primer sets: 5'-CCTACTA-CCTGGAGAACG-3' and 5'-GCTGGACACATATAGTCG-3' for the detection of ESRα and 5'-AGCCATGACATTCTAT-AGC-3' and 5'-CCACTTCGTAACACTTCC-3' for ESRβ.

GST Pull-down Assay—The GST pull-down assay was conducted as described previously (25).

Immunoprecipitation Analysis—Immunoprecipitation analysis was performed as described previously (25). The antibodies
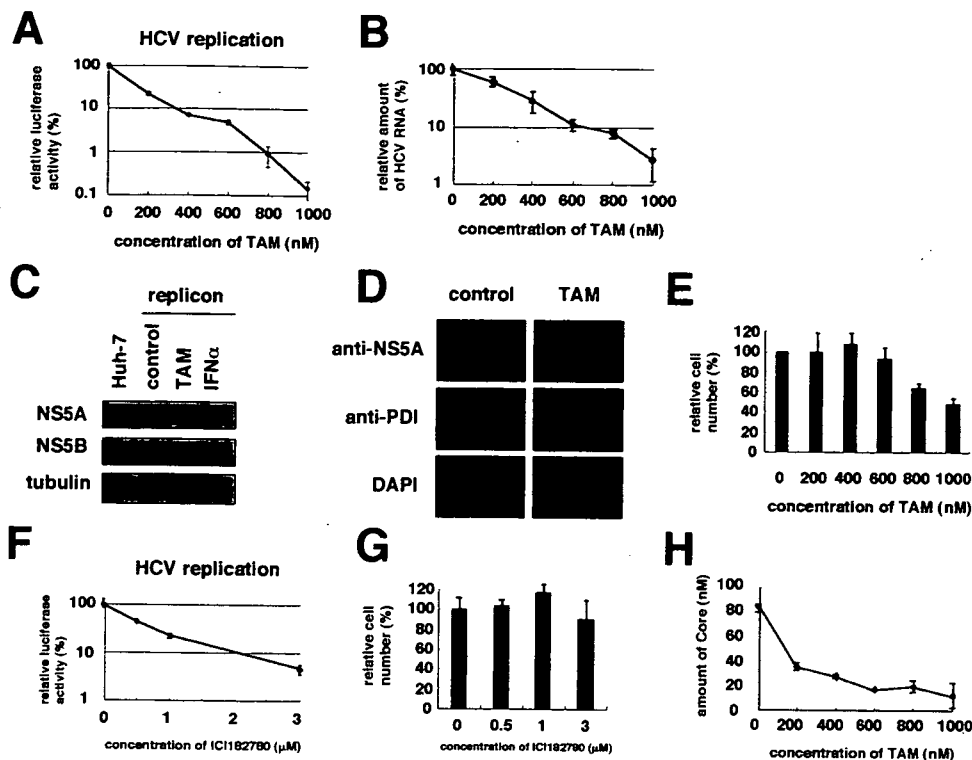
FIGURE 1. **TAM suppressed the replication of the HCV genome.** A, luciferase activities were measured using the LucNeo#2 cells, which carried a luciferase-containing replicon RNA, upon treatment with TAM at the indicated doses for 7 days. Relative luciferase activities are plotted against the concentrations of TAM. The data show the means of three independent experiments. The *error bars* are indicated. B, HCV RNA was quantified by real time RT-PCR analysis using the lysates from MH-14 cells, harboring the HCV subgenomic replicon, treated with the indicated doses of TAM for 7 days. Relative amounts of HCV RNA are shown. C, HCV NS5A and NS5B proteins as well as tubulin as an internal control were detected by immunoblot analysis in the lysates from MH-14 cells (replicon) treated without (control) or with 500 nM TAM or 100 IU/ml interferon-α as a positive control for 7 days and Huh-7 cells. D, HCV NS5A and protein-disulfide isomerase (PDI) as an internal control were detected by indirect immunofluorescence analysis in the cells treated without (control) or with 500 nM TAM for 7 days. 4′,6-Diamidino-2-phenylindole (DAPI) shows a nuclear staining. E, cell number was counted after 5 days upon treatment with various concentrations of TAM. Relative cell numbers are shown. F, luciferase activities with LucNeo#2 cells treated with various concentrations of ICI182780 were measured as described in A. G, cell number was counted under treatment with ICI182780 at the indicated concentrations. H, core in the culture medium of JFH1 RNA-transfected cells upon treatment with TAM was quantified as described under "Experimental Procedures."

RESULTS

Tamoxifen Suppressed HCV Genome Replication—We screened for agents that suppressed HCV genome replication using a HCV subgenomic replicon system (13, 16). Among the compounds tested, we observed that TAM inhibited HCV genome replication. HCV replication activity, monitored by luciferase activity (22), and the amount of HCV RNA were decreased with TAM treatment in a dose-dependent manner (Fig. 1, A and B). The expression of HCV proteins, NS5A and NS5B, detected by immunoblot (Fig. 1C) and indirect immuofluorescence analyses (Fig. 1D), also drastically decreased by treatment with TAM. A high concentration of TAM decreased cell proliferation (Fig. 1E). However, TAM suppressed HCV replication without any cytotoxicity in another cell line, HuS-E7/DN24 cells (Fig. 6, C and D). In addition, a pure anti-estrogen compound ICI182780, which had little cytotoxic effect, reduced HCV RNA (Fig. 1, F and G). Moreover, TAM inhibited the production of core in the culture medium of HCV JFH1-transfected cells, in a recently developed system of the production of infectious HCV particles (Fig. 1H) (28–30). The above data indicate that TAM suppresses HCV genome replication.

ESR Was Involved in HCV Genome Replication—Next, we investigated which cellular protein TAM targets to suppress HCV replication. It has been reported that TAM targets 1) ESR (31), 2) P-glycoprotein (32, 33), 3) calmodulin (34), 4) protein kinase C (35, 36), etc. Although other compounds targeting P-glycoprotein, calmodulin, and protein kinase C did not affect HCV replication in our screening (data not shown), ESR was suggested to play a role in HCV replication as shown below.

RNAi-mediated specific knockdown of endogenous ESRα and ESRβ (Fig. 2A) reduced HCV RNA in replicon-containing cells to ~20–40% and 60–70%, respectively (Fig. 2B). Transient transfection with ESRα and ESRβ expression plasmids, which activated ERE-driven transcription 4–5-fold (Fig. 2C), showed that ectopically expressed ESRα augmented HCV replication activity in a dose-dependent manner, whereas ESRβ did not (Fig. 2D). ESRα-induced augmentation of the replication was reversed upon TAM treatment (Fig. 2D). These results suggested a significant role of ESR, especially ESRα, in HCV

used in this study were mouse normal IgG as a negative control (Zymed Laboratories), anti-NS5B (anti-NS5B#10; a generous gift from Dr. Kohara at the Tokyo Metropolitan Institute of Medical Science), anti-FLAG, and anti-caveolin-2 antibodies.

Fractionation of Cell Extracts—MH-14 cells transfected with the expression plasmid for FLAG-tagged ESRα were fractionated essentially as described previously (25).

HCV Replication Complex Assay—Isolation of HCV RC was done as described previously (16, 21).

In Vitro HCV Infection Experiment—In vitro HCV infection was conducted essentially as described (23). Briefly, HCV-infected serum (~2 × 10⁵ copies) was inoculated into HuS-E7/DN24 cells (5 × 10⁴ cells) for 24 h. After washes, cells were cultured in the medium supplemented with 10 μM PD98059 to stimulate HCV translation (27) (*scheme* in Fig. 6B). To observe HCV amplification, HCV RNA in the cells was quantified, since HCV RNA was hardly detected significantly in the culture medium (23).

3-(4,5-Dimethylthiazol-2-yl)-2,5-diphenyltetrazolium bromide Assay—The 3-(4,5-dimethylthiazol-2-yl)-2,5-diphenyltetrazolium bromide assay was performed to examine the
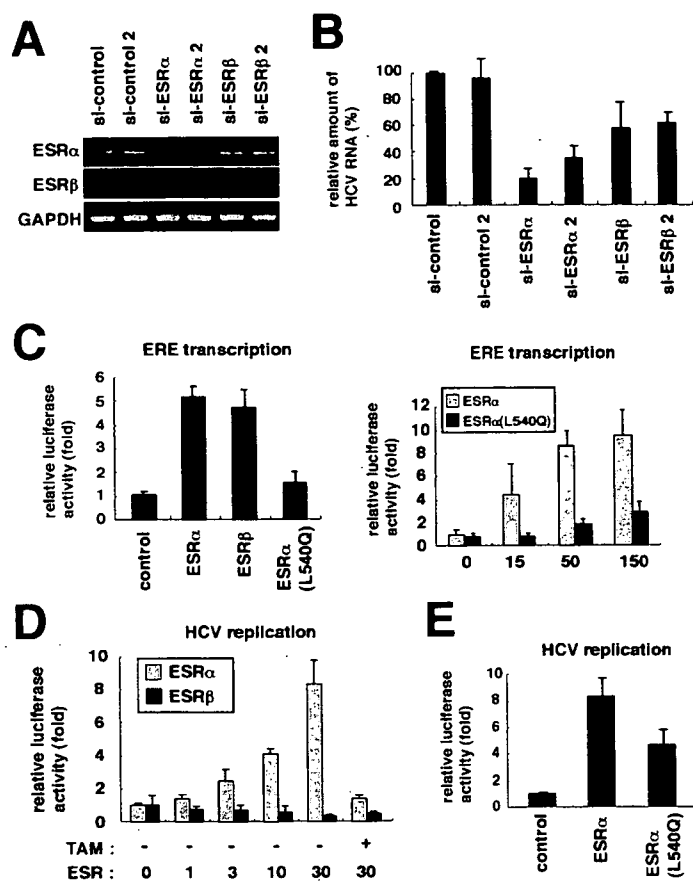
FIGURE 2. ESR was involved in HCV genome replication. *A*, specific knockdown of endogenous ESRα and ESRβ. RT-PCR analysis was performed to detect the expression of ESRα, ESRβ, and glyceraldehyde-3-phosphate dehydrogenase (*GAPDH*) as an internal control in the cells transfected with siRNA recognizing ESRα (si-ESRα, si-ESRα2), ESRβ (si-ESRβ, si-ESRβ2), or randomized siRNA (si-control, si-control2). *B*, HCV RNA was quantified as shown in Fig. 1*B*, using the cells transfected with si-control, si-control2, si-ESRα, si-ESRα2, si-ESRβ, and si-ESRβ2 for 5 days. *C*, the ERE-mediated transcriptional activities were measured by a luciferase assay using the lysates from the cells transfected with pGL3-EREX3-TATA-Luc reporter plasmid together with pcDNA3-ERα (ESRα), pcDNA3-hERβ (ESRβ), pcDNA-ESRα(L540Q), or the empty vector (control) (*left*) or varying amounts (ng) of pcDNA3-ERα (ESRα) or pcDNA-ESRα(L540Q) (*right*) and treated with 100 nm estradiol for 36 h. *D* and *E*, HCV replication activities were examined by quantifying the luciferase activities using cured MH-14 cells transfected with the indicated doses (ng) of ESRα or ESRβ (*D*) or 30 ng of ESRα, ERα(L540Q), or the empty vector (control) (*E*) together with 0.125 μg of LMH14 RNA without or with 1 μM TAM for 4 days.

genome replication. ESRα(L540Q), carrying a leucine to glutamine point mutation at aa 540 within the L*XX*LL motif (aa 536–540) of ESRα (37), had much lower transactivation activity driven from ERE (Fig. 2*C*). However, ESRα(L540Q) stimulated HCV replication activity ~5-fold, although the stimulation was less than that by wild-type ESRα (Fig. 2*E*). Thus, ESRα having lower transactivating capacity could still facilitate HCV replication.

ESRα Interacted with HCV NS5B—Thus, the chemical biology approach revealed the involvement of ESR in HCV genome replication. Then we investigated the molecular mechanism of ESR-induced HCV replication. A binding assay between ESRα and HCV proteins expressed in the HCV subgenomic replicon showed that the C domain of ESRα coprecipitated with NS5B but not NS3, NS4B, and NS5A (Fig. 3*A*). Other ESRα domains, A/B, D, and E/F, did not bind to any HCV proteins. A coimmunoprecipitation assay also indicated the presence of ESRα in the
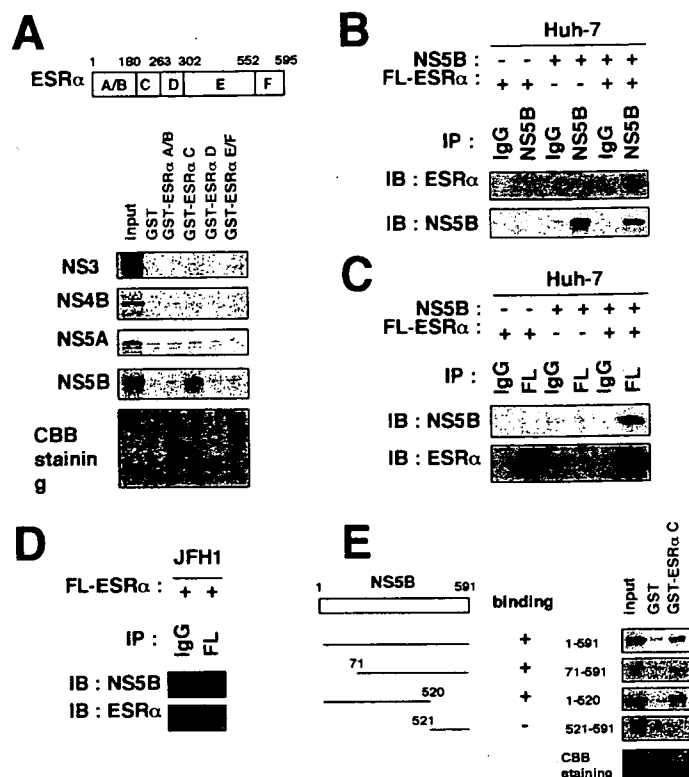

FIGURE 3. ESRα interacted with HCV NS5B. *A, top,* schematic representation of the primary structure of ESRα. ESRα consists of domains A–F. The amino acid numbers are also shown. *Bottom,* GST pull-down assays were performed using the recombinant proteins of the A/B, C, D, and E/F domain of ESRα fused with GST and *in vitro* translated HCV NS3, NS4B, NS5A, and NS5B protein. *Input,* the one-fifth amount of protein used for the pull-down assay. The Coomassie Brilliant Blue staining pattern of the precipitated fraction is also shown in the *bottom panel*. *B–D,* the lysates from the cells ectopically expressing NS5B (*B* and *C*) or the whole open reading frame of the HCV JFH1 strain (*D*) and/or FLAG-tagged ESRα were immunoprecipitated (*IP*) with anti-NS5B (*B*; NS5B), anti-FLAG antibody (*C* and *D*; FL), or mouse normal IgG as a negative control followed by the detection of ESRα and NS5B by immunoblot analysis (*IB*). *E,* deletion mutants of NS5B were subjected to a GST pull-down assay with GST-fused C domain of ESRα as described in *A*. The *left panel* shows a schematic representation of the full-length and truncated mutants of NS5B. The *numbers* indicate the amino acid numbers in NS5B.

immunoprecipitate by anti-NS5B antibody (Fig. 3, *B* and *D*), and *vice versa* (Fig. 3*C*). Thus, ESRα specifically interacted with NS5B. Deletion analysis indicated that the region of 71–591 and 1–520 but not 521–591 of NS5B coprecipitated with the recombinant C domain of ESRα (Fig. 3*E*). This binding profile is different from that between cyclophilin B and NS5B, which we previously reported (21).

The ESRα-NS5B Interaction Was Important for the Regulation of HCV Genome Replication—To examine whether the interaction between ESRα and NS5B was essential for the ESRα-mediated regulation of HCV replication or not, we searched for a point mutant of ESRα that could not bind to NS5B by alanine-scanning mutation analysis. ESRα mutants, ESRα(255M) and ESRα(258M), in which IRK at aa 255–257 and DRR at aa 258–260 was replaced by TGT and AQT, respectively, had little affinity with NS5B (Fig. 4*A*) but still possessed the ERE-mediated transactivation capacity (Fig. 4*B*). However, both ESRα(255M) and ESRα(258M) caused only weak activations of HCV replication, compared with wild type ESRα (Fig. 4*C*). The data suggest that the interaction of ESRα with NS5B is
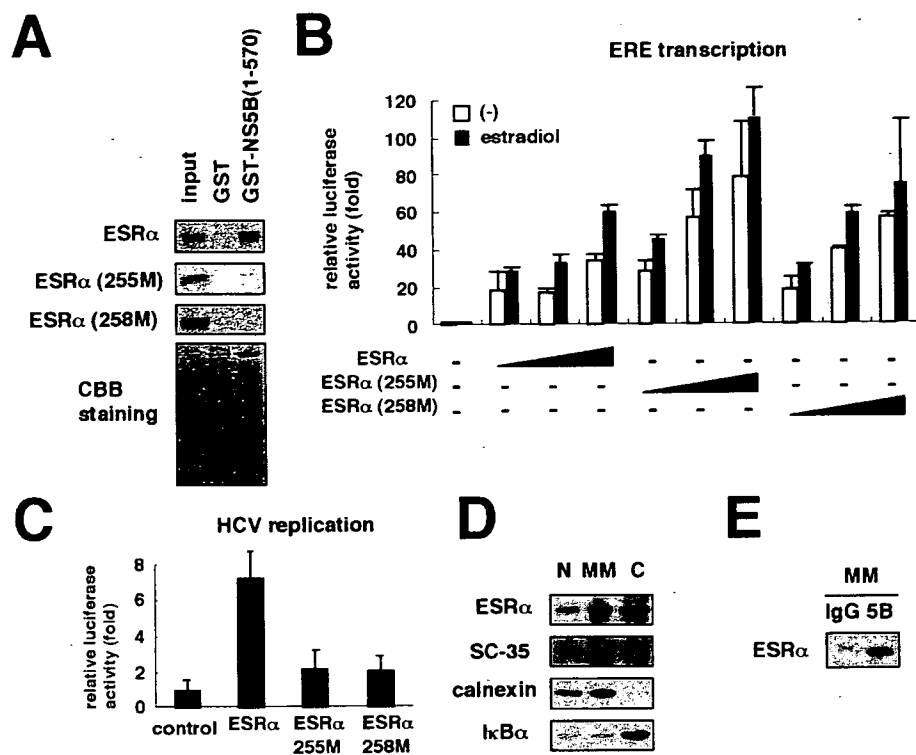
A

Input
GST
GST-NS5B(1-570)

ESRα

ESRα (255M)

ESRα (258M)

CBB staining

B

ERE transcription

□ (-)
■ estradiol

relative luciferase activity (fold)

120
100
80
60
40
20
0

ESRα
ESRα (255M)
ESRα (258M)

C

HCV replication

relative luciferase activity (fold)

8
6
4
2
0

control   ESRα   ESRα   ESRα
                  255M   258M

D

N MM C

ESRα

SC-35

calnexin

IκBα

E

MM

IgG 5B

ESRα

FIGURE 4. **The interaction of NS5B mediated the regulation of HCV genome replication by ESRα.** *A*, GST pull-down assays were performed as described in Fig. 3*A* using the wild type ESRα or point mutant of ESRα, ESRα(255M), and ESRα(258M). *B*, the mutation within ESRα(255M) and ESRα(258M) did not reduce the activation capacity of ERE-mediated transcription. Huh-7 cells were transfected with the expression plasmids for ESRα, ESRα(255M), or ESRα(258M) at doses of 10, 30, and 100 ng each together with pGL3-EREX3-TATA-Luc reporter plasmid and treated without (*white bar*) or with 100 nм estradiol (*black bar*) to quantify the luciferase activity. *C*, HCV replication activities were examined by quantifying the luciferase activities as described in the legend to Fig. 2*D* in the cells upon transfection with the expression plasmids for wild type ESRα, ESRα(255M), or ESRα(258M). *D*, the cells were fractionated into the nucleus (*N*), MM, and cytoplasm (*C*). Each fraction was detected for FLAG-tagged ESRα, SC-35, calnexin, and IκBα, respectively, by immunoblot analysis. Calnexin, an ER marker protein, was detected in the nucleus as well as MM, probably because of the existence of the nuclear membrane in the nuclear fraction. *E*, the MM fraction obtained in *D* was subjected to a coimmunoprecipitation assay using anti-NS5B or IgG followed by immunoblot analysis for the detection for ESRα.

critical for ESRα-mediated regulation of HCV genome replication.

Thus, ESRα interaction with NS5B regulates HCV replication. NS5B is mainly located on the cytoplasmic surface of the ER membrane (21, 38). On the other hand, ESRα as a nuclear hormone receptor is normally distributed in the cytoplasm and translocates into the nucleus upon ligand stimulation. In addition, a part of ESRα localizes on the membrane fraction. In our experiment, NS5B was mainly located around the ER, colocalized with the ER marker, protein-disulfide isomerase (data not shown) (21). Ectopically expressed ESRα showed diffuse distribution in the cells (data not shown). We fractionated cell homogenates and observed that a part of the ESRα resided in the microsomal membrane (MM) fraction (Fig. 4*D*). Moreover, ESRα in the MM fraction was coprecipitated with NS5B (Fig. 4*E*). It suggests the possibility that the interaction between NS5B and ESRα, at least in part of them, occurs on the ER membrane.

ESRα Promoted the Participation of NS5B in the HCV Replication Complex—It was reported that HCV proteins involved in the replication machinery was associated with the lipid raft on the ER and cofractionated with CAV2. A coimmunoprecipitation assay showed that NS5B associated with CAV2 (Fig. 5*A*).

In the experiment investigating the role of ESRα in NS5B-CAV2 association, the coprecipitation of NS5B with CAV2 was decreased upon the knocking down of ESRα (Fig. 5*B*). Treatment with TAM abrogated the association of NS5B with CAV2 (Fig. 5*C*), although the total amount of NS5B in the cells is similar in the presence and absence of TAM for 24 h in this experiment (data not shown). Thus, ESRα was suggested to promote the association between NS5B and CAV2. Since a part of CAV2 resided on the lipid raft on the ER (18), ESRα-mediated binding between NS5B and CAV2 was possible to affect the localization of NS5B to the HCV RC. To see the consequential relevance of ESRα on NS5B function, we analyzed the HCV RC by treatment with digitonin/protease as described previously (16). HCV proteins involved in the RC and surrounded by the membrane structure are resistant to the treatment with digitonin followed by protease, whereas those unrelated to the replication outside the RC are digested by the treatment. By using this technique measuring the sensitivity to protease, HCV RC can be distinguished from the ER that is not related to the replication, although the RC and the nucleus cannot be separated. The experimental condition for fractionation was confirmed with the detection with IκBα and calnexin; a cytosolic protein IκBα was washed out following the treatment with digotinin (Fig. 5*D*, *lanes 1* and *2*), and ER protein calnexin, which did not accumulate in the RC, was digested by treatment with digotinin/protease (Fig. 5*D*, *lanes 2– 4*). An ER lipid raft component, CAV2, was still detected under the digitonin/protease treatment (the RC-containing fraction) (Fig. 5*D*, *lanes 3* and *4*). Under this condition, a part of NS5B was detected in the digitonin/protease-resistant fraction, as described previously (16) (Fig. 5*D*, *lanes 3* and *4*). However, NS5B in this fraction was decreased upon treatment with TAM (Fig. 5*D*, *lanes 3, 4, 7*, and *8*). On the other hand, the amount of NS5A was not significantly changed by TAM treatment. Knocking down of ESRα also disrupted the association of NS5B with the RC-containing fraction (Fig. 5*E*). From the above results, it was suggested that ESRα promoted the participation of NS5B in the RC (also see "Discussion").

ESRα Could Serve as a Molecular Target of Anti-HCV Agents— Finally, we assessed the possibility that the association of ESRα with NS5B could serve as a target of anti-HCV agents. By introducing a decoy peptide against ESRα-NS5B interaction, consisting of the C domain of ESRα into replicon-bearing cells,
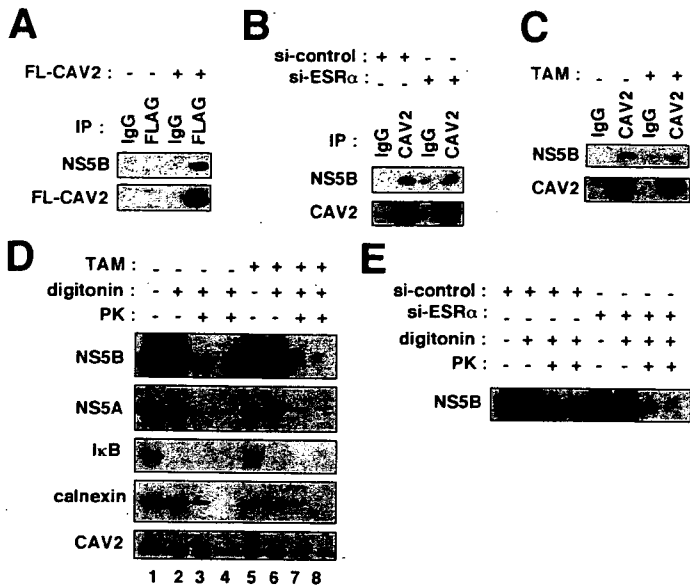
A **B** **C**

FIGURE 5. **ESRα promoted the participation of NS5B in HCV RC.** *A–C*, a coimmunoprecipitation assay (*IP*) was performed with anti-FLAG (*A*), anti-CAV2 (*B* and *C*) antibody, or mouse normal IgG from the lysates of the cells transfected without or with FLAG-tagged CAV2 (*A*), transfected with si-control or si-ESRα (*B*), or treated without or with 1 μM TAM (*C*). NS5B (*top*) and CAV2 (*bottom*) were detected by immunoblot analysis. *D*, detection of the amount of NS5B in the digitonin/protease-resistant fraction. MH-14 cells were treated without (*lanes 1–4*) or with 1 μM TAM (*lanes 5–8*) for 24 h. Cells were then treated without (*lanes 1* and *5*) or with digitonin (*lanes 2–4* and *6–8*), followed by digestion with proteinase K (0 μg/ml for *lanes 2* and *6*, 0.3 μg/ml for *lanes 3* and *7*, and 1 μg/ml for *lanes 4* and *8*). NS5B, NS5A, IκBα, calnexin, and CAV2 were detected by immunoblot analysis. *E*, HCV RC was isolated as described in *D* using the cells transfected with si-control or si-ESRα, and NS5B was detected. A similar result was obtained by using si-ESRα2.

HCV replication activity was reduced in a dose-dependent manner (Fig. 6*A*). To further observe the significance of ESRα in a physiological condition, we performed an *in vitro* infection experiment using serum from an HCV-infected patient as a nascent virus inoculum and nonneoplastic human hepatocytes as highly infection-permissive cells (Fig. 6*B*). Treatment with 1 μM TAM did not show a cytotoxic effect on these cells in any time course examined (Fig. 6*C*). However, treatment with TAM as well as cyclosporin A as a positive control inhibited the multiplication of viral genome RNA in the cells along with the time course (Fig. 6*D*). Thus, ESRα could serve as a potent molecular target of anti-HCV agents.

DISCUSSION

In general, viruses take advantage of host cell factors for their replication. So far, some factors have been shown to relevantly regulate HCV replication, including hVAP33 (39, 40), FBL2 (41), and cyclophilin B (21). Among these, FBL2 and cyclophilin B were identified by a chemical biological approach; FBL2 from the observation of an anti-HCV activity of lovastatin and an inhibitor of geranylgeranyl transferase (41–43); cyclophilin B from the inhibitory effect of cyclosporin A on HCV replication (20, 21). In this study, we found a suppressive capacity of TAM to HCV genome replication. Through further examination using TAM, we revealed ESRα as a host cell factor regulating HCV replication and suggested its regulation mechanism.

Currently, it is proposed that HCV RC that replicates the HCV genome is formed on the intracellular membrane, including the ER membrane (14–17). It was also reported that HCV genome replication was associated with the lipid raft on the intracellular membrane (18). Most HCV proteins are not related to the RC, whereas only a minor portion of HCV proteins take part in the RC to drive the viral replication (16). It has remained widely unknown, however, how HCV proteins are regulated to participate in the RC. It was reported that hVAP-33 binds to NS5A and NS5B, and this protein is related to the amount of NS5B in the lipid raft (40). hVAP-33 was speculated to recruit NS5B to the lipid raft, although its molecular mechanism has not been analyzed. This study suggested the interaction between ESRα and NS5B in the ER fraction, although we did not show the existence of ESRα in the RC, since the RC and the nucleus cannot be separated in the digitonin/protease treatment experiment. ESRα promoted the interaction of NS5B with CAV2. Previous papers reported that ESRα bound to CAV1 and CAV2 (6). From these observations, ESRα is
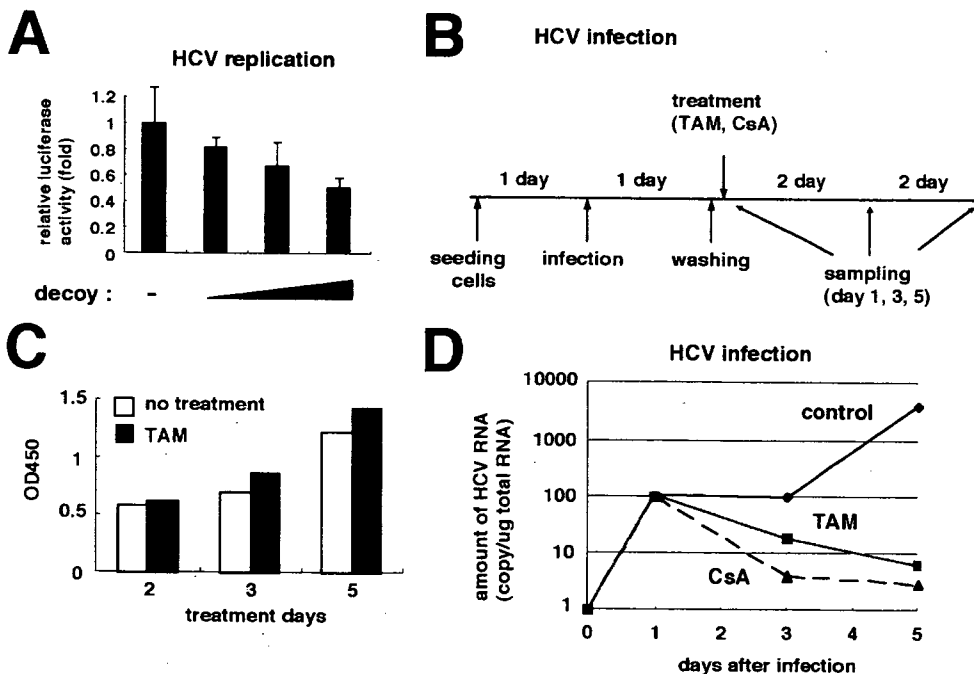
A **B**

C **D**

FIGURE 6. **ESRα could serve as a molecular target for anti-HCV agents.** *A*, HCV replication activity was measured by quantifying the luciferase activity as described in the legend to Fig. 2*D* in the cells overexpressing a decoy peptide consisting of the C domain of ESRα. *B*, experimental scheme of *in vitro* HCV infection experiment. After seeding the HuS-E7/DN24 cells, HCV-positive serum was inoculated for 24 h. After extensive washes, the cells were cultured with the medium supplemented without (control) or with 1 μM TAM or 3 μg/ml cyclosporin A. HCV genome RNA was quantified along with the time course (days 1, 3, and 5 postinoculation) by real time RT-PCR analysis. *C*, the treatment with 1 μM TAM did not show any cytotoxic effect on HuS-E7/DN24 cells. 3-(4,5-Dimethylthiazol-2-yl)-2,5-diphenyltetrazolium bromide assays were performed as described under "Experimental Procedures" to examine the viability of the cells at days 2, 3, and 5 postinoculation. *D*, HCV genome RNA was quantified as described in *B* and plotted against the time course.

likely to function as a bridging factor that connects NS5B to CAV2, although we cannot fully neglect the possibility that ESRα augments NS5B-CAV2 binding via another function, such as transcriptional activity. Because CAV2 resided on the lipid raft of the intracellular membrane (18), this action of ESRα may recruit NS5B to the lipid raft and the HCV RC. In fact, ESRα promoted the participation of NS5B in the HCV RC. Thus, ESRα is suggested to escort NS5B to the HCV RC, although it is also possible that ESRα augments the number of the RC itself. However, ESRα at least augments the amount of NS5B involved in HCV replication machinery to stimulate the replication. It was reported that the membrane-associated ESRα served as a platform where signalsomes, including receptor tyrosine kinase, nonreceptor tyrosine kinase Src, and G proteins, assembled and activated downstream signaling pathways (44–46). HCV may also take advantage of such platform characteristics of ESRα to form the RC for their efficient replication. Although the mechanisms of the nuclear receptor function of ESRα have been extensively elucidated, the functions of membrane-associated ESRα have not been widely characterized so far. This study suggested a novel physiological relevance of membrane-associated ESRα as a regulator of the viral replication.

Until now, there are no clinical studies that report a direct interaction of TAM treatment with HCV replication in patients infected with HCV. Given our results, examinations on the effect of TAM or other anti-estrogen drugs may be one of the useful approaches to develop a new anti-HCV strategy. On the other hand, we disclosed the mechanism of ESR-mediated regulation of HCV genome replication. Screening for compounds that inhibit this mechanism expectedly led to novel types of anti-HCV agents. Further analyses on ESR are needed to develop anti-HCV therapeutics as well as reveal the regulation mechanism of HCV replication.

REFERENCES

1. Mangelsdorf, D. J., Thummel, C., Beato, M., Herrlich, P., Schutz, G., Umesono, K., Blumberg, B., Kastner, P., Mark, M., Chambon, P., and Evans, R. M. (1995) *Cell* **83**, 835–839
2. Acconcia, F., and Kumar, R. (2006) *Cancer Lett.* **238**, 1–14
3. Levin, E. R. (2005) *Mol. Endocrinol.* **19**, 1951–1959
4. Song, R. X., Zhang, Z., and Santen, R. J. (2005) *Trends Endocrinol. Metab.* **16**, 347–353
5. Razandi, M., Alton, G., Pedram, A., Ghonshani, S., Webb, P., and Levin, E. R. (2003) *Mol. Cell. Biol.* **23**, 1633–1646
6. Razandi, M., Oh, P., Pedram, A., Schnitzer, J., and Levin, E. R. (2002) *Mol. Endocrinol.* **16**, 100–115
7. Marquez, D. C., Chen, H. W., Curran, E. M., Welshons, W. V., and Pietras,
R. J. (2006) *Mol. Cell. Endocrinol.* **246**, 91–100
8. Liang, T. J., Jeffers, L. J., Reddy, K. R., De Medina, M., Parker, I. T., Cheinquer, H., Idrovo, V., Rabassa, A., and Schiff, E. R. (1993) *Hepatology* **18**, 1326–1333
9. Grakoui, A., Wychowski, C., Lin, C., Feinstone, S. M., and Rice, C. M. (1993) *J. Virol.* **67**, 1385–1395
10. Hijikata, M., Kato, N., Ootsuyama, Y., Nakagawa, M., and Shimotohno, K. (1991) *Proc. Natl. Acad. Sci. U. S. A.* **88**, 5547–5551
11. Bartenschlager, R., and Lohmann, V. (2001) *Antiviral Res.* **52**, 1–17
12. Tellinghuisen, T. L., and Rice, C. M. (2002) *Curr. Opin. Microbiol.* **5**, 419–427
13. Lohmann, V., Korner, F., Koch, J., Herian, U., Theilmann, L., and Bartenschlager, R. (1999) *Science* **285**, 110–113
14. Aizaki, H., Lee, K. J., Sung, V. M., Ishiko, H., and Lai, M. M. (2004) *Virology* **324**, 450–461
15. Egger, D., Wolk, B., Gosert, R., Bianchi, L., Blum, H. E., Moradpour, D., and Bienz, K. (2002) *J. Virol.* **76**, 5974–5984
16. Miyanari, Y., Hijikata, M., Yamaji, M., Hosaka, M., Takahashi, H., and Shimotohno, K. (2003) *J. Biol. Chem.* **278**, 50301–50308
17. Moradpour, D., Gosert, R., Egger, D., Penin, F., Blum, H. E., and Bienz, K. (2003) *Antiviral Res.* **60**, 103–109
18. Shi, S. T., Lee, K. J., Aizaki, H., Hwang, S. B., and Lai, M. M. (2003) *J. Virol.* **77**, 4160–4168
19. Watashi, K., and Shimotohno, K. (2007) *Rev. Med. Virol.* **17**, 245–252
20. Watashi, K., Hijikata, M., Hosaka, M., Yamaji, M., and Shimotohno, K. (2003) *Hepatology* **38**, 1282–1288
21. Watashi, K., Ishii, N., Hijikata, M., Inoue, D., Murata, T., Miyanari, Y., and Shimotohno, K. (2005) *Mol. Cell* **19**, 111–122
22. Goto, K., Watashi, K., Murata, T., Hishiki, T., Hijikata, M., and Shimotohno, K. (2006) *Biochem. Biophys. Res. Commun.* **343**, 879–884
23. Aly, H. H., Watashi, K., Hijikata, M., Kaneko, H., Takada, Y., Egawa, H., Uemoto, S., and Shimotohno, K. (2007) *J. Hepatol.* **46**, 26–36
24. Hino, H., Tateno, C., Sato, H., Yamasaki, C., Katayama, S., Kohashi, T., Aratani, A., Asahara, T., Dohi, K., and Yoshizato, K. (1999) *Biochem. Biophys. Res. Commun.* **256**, 184–191
25. Watashi, K., Hijikata, M., Tagawa, A., Doi, T., Marusawa, H., and Shimotohno, K. (2003) *Mol. Cell. Biol.* **23**, 7498–7509
26. Murata, T., Ohshima, T., Yamaji, M., Hosaka, M., Miyanari, Y., Hijikata, M., and Shimotohno, K. (2005) *Virology* **331**, 407–417
27. Murata, T., Hijikata, M., and Shimotohno, K. (2005) *Virology* **340**, 105–115
28. Lindenbach, B. D., Evans, M. J., Syder, A. J., Wolk, B., Tellinghuisen, T. L., Liu, C. C., Maruyama, T., Hynes, R. O., Burton, D. R., McKeating, J. A., and Rice, C. M. (2005) *Science* **309**, 623–626
29. Wakita, T., Pietschmann, T., Kato, T., Date, T., Miyamoto, M., Zhao, Z., Murthy, K., Habermann, A., Krausslich, H. G., Mizokami, M., Bartenschlager, R., and Liang, T. J. (2005) *Nat. Med.* **11**, 791–796
30. Zhong, J., Gastaminza, P., Cheng, G., Kapadia, S., Kato, T., Burton, D. R., Wieland, S. F., Uprichard, S. L., Wakita, T., and Chisari, F. V. (2005) *Proc. Natl. Acad. Sci. U. S. A.* **102**, 9294–9299
31. Shang, Y. (2006) *Nat. Rev. Cancer* **6**, 360–368
32. Callaghan, R., and Higgins, C. F. (1995) *Br. J. Cancer* **71**, 294–299
33. Raderer, M., and Scheithauer, W. (1993) *Cancer* **72**, 3553–3563
34. Lopes, M. C., Vale, M. G., and Carvalho, A. P. (1990) *Cancer Res.* **50**, 2753–2758
35. O'Brian, C. A., Liskamp, R. M., Solomon, D. H., and Weinstein, I. B. (1985) *Cancer Res.* **45**, 2462–2465
36. O'Brian, C. A., Ward, N. E., and Anderson, B. W. (1988) *J. Natl. Cancer Inst.* **80**, 1628–1633
37. Leers, J., Treuter, E., and Gustafsson, J. A. (1998) *Mol. Cell. Biol.* **18**, 6001–6013
38. Schmidt-Mende, J., Bieck, E., Hugle, T., Penin, F., Rice, C. M., Blum, H. E., and Moradpour, D. (2001) *J. Biol. Chem.* **276**, 44052–44063
39. Evans, M. J., Rice, C. M., and Goff, S. P. (2004) *Proc. Natl. Acad. Sci. U. S. A.* **101**, 13038–13043
40. Gao, L., Aizaki, H., He, J. W., and Lai, M. M. (2004) *J. Virol.* **78**, 3480–3488
41. Wang, C., Gale, M., Jr., Keller, B. C., Huang, H., Brown, M. S., Goldstein, J. L., and Ye, J. (2005) *Mol. Cell* **18**, 425–434

42. Kapadia, S. B., and Chisari, F. V. (2005) *Proc. Natl. Acad. Sci. U. S. A.* **102,** 2561–2566

43. Ye, J., Wang, C., Sumpter, R., Jr., Brown, M. S., Goldstein, J. L., and Gale, M., Jr. (2003) *Proc. Natl. Acad. Sci. U. S. A.* **100,** 15865–15870

44. Migliaccio, A., Piccolo, D., Castoria, G., Di Domenico, M., Bilancio, A., Lombardi, M., Gong, W., Beato, M., and Auricchio, F. (1998) *EMBO J.* **17,** 2008–2018

45. Razandi, M., Pedram, A., Greene, G. L., and Levin, E. R. (1999) *Mol. Endocrinol.* **13,** 307–319

46. Wyckoff, M. H., Chambliss, K. L., Mineo, C., Yuhanna, I. S., Mendelsohn, M. E., Mumby, S. M., and Shaul, P. W. (2001) *J. Biol. Chem.* **276,** 27071–27076

ELSEVIER

Liver target delivery of small interfering RNA to the HCV gene by lactosylated cationic liposome☆

Tsunamasa Watanabe[1,2,†], Takuya Umehara[1,†,‡], Fumihiko Yasui[1],
Shin-ichiro Nakagawa[1,3], Junichi Yano[3], Tadaaki Ohgi[3], Satoru Sonoke[3],
Kenichi Satoh[1,4], Kazuaki Inoue[1,2], Makoto Yoshiba[2], Michinori Kohara[1,*]

[1]Department of Microbiology and Cell Biology, The Tokyo Metropolitan Institute of Medical Science, 3-18-22 Honkomagome,
Bunkyo-ku, Tokyo 113-8613, Japan
[2]Division of Gastroenterology, Showa University Fujigaoka Hospital, 1-30 Fujigaoka, Aoba-ku, Yokohama 227-8501, Japan
[3]Discovery Research Laboratories, Nippon Shinyaku Co. Ltd., 14 Nishinosho-monguchi-cho, Kisshoin, Minami-ku, Kyoto 601-8550, Japan
[4]Division of Gastroenterology and Hepatology, Department of Internal Medicine, The Jikei University School of Medicine, 3-25-8 Nishi-shimbashi,
Minato-ku, Tokyo 105-8461, Japan

Background/Aims: RNA interference has considerable therapeutic potential, particularly for anti-viral therapy. We previously reported that hepatitis C virus (HCV)-directed small interfering RNA (siRNA; siE) efficiently inhibits HCV replication, using HCV replicon cells. To employ the siRNA as a therapeutic strategy, we attempted *in vivo* silencing of intrahepatic HCV gene expression by siE using a novel cationic liposome.

Methods: The liposomes consisted of conjugated lactose residues, based on the speculation that lactose residues would effectively deliver siRNA to the liver *via* a liver specific receptor. The lactosylated cationic liposome 5 (CL-LA5) that contained the most lactose residues introduced the most siRNA into a human hepatoma cell line, which then inhibited replication of HCV replicons.

Results: In mice, the siRNA/CL-LA5 complexes accumulated primarily in the liver and were widespread throughout the hepatic parenchymal cells. Moreover, siE/CL-LA5 specifically and dose-dependently suppressed intrahepatic HCV expression in transgenic mice without an interferon response.

Conclusions: The present results indicate that the CL-LA5 we developed is a good vehicle to lead siRNA to the liver. Hence, CL-LA5 will be helpful for siRNA therapy targeting liver diseases, especially hepatitis C.

© 2007 European Association for the Study of the Liver. Published by Elsevier B.V. All rights reserved.

Keywords: siRNA; HCV; Cationic liposome; Lactosylation; Target delivery; Hepatocyte; Liver; Transgenic mouse; Interferon

1. Introduction

Hepatitis C virus (HCV) is a major etiological agent that causes chronic hepatitis, liver cirrhosis, and hepatocellular carcinoma [1]. Although combination therapy with pegylated interferon-α and ribavirin has markedly improved the clinical outcome, less than half of the patients with chronic hepatitis C can be expected to respond favourably to currently available agents [2]. Therefore, developing a specific reagent against HCV is a major public health objective.

RNA interference (RNAi) is one type of post-transcriptional gene silencing [3,4]. The effector of RNAi is

short interfering RNA (siRNA) duplexes (~21–23 nt), which play a key role in the specific degradation of target mRNA. Currently, RNAi technology is widely used as a tool for gene function analysis. In addition, it is expected to be a powerful therapeutic agent to silence pathogenic gene products associated with disease, including cancer, viral infections and autoimmune disorders [5–10]. Previously, we and others reported that synthetic siRNA efficiently and specifically inhibits HCV replication in vitro [11–20] and suggested the potential for siRNA as a novel HCV agent.

In fact, the RNAi machinery has been shown to work in vivo by injection of siRNA [21]. However, safety and delivery remain the main obstacles to achieving in vivo gene silencing by RNAi technology. Currently, viral vectors [22], hydrodynamic injection [23] and cationic liposomes [24] have been the main methods of introducing siRNA in vivo. However, the mechanism of action of viral vectors has not been clarified and may result in severe side effects. Furthermore, hydrodynamic injection cannot be used for human therapy. On the other hand, since the physical properties of cationic liposomes are well understood, the use of these liposomes holds the best promise for clinical application. In addition, cationic liposomes do not elicit an immune response, which is a great advantage for drug targeting in that multiple administrations of siRNA are possible, which is crucial for an siRNA therapeutic effect. Moreover, cationic liposomes are easily modified and improved.

In HCV therapy, it is important that reagents are specifically led to the liver. Thus, to specifically and effectively transfer siRNA into hepatocytes, we designed lactosylated cationic liposomes, as Ohishi et al. reported that lactosylated polyion complex micelles enhanced the delivery of oligonucleotides into hepatoma cells [25]. Based on their observations we expected that siRNA complexed with lactosylated cationic liposomes would be superficially trapped in the liver by lactose-specific receptors and therefore effectively introduced into hepatic parenchymal cells in vivo.

Here, we report that siRNAs with cationic liposomes containing lactose residues were largely transfected into hepatocytes in vitro and in vivo, where they efficiently suppressed intrahepatic HCV expression in transgenic mice. Furthermore, this system did not activate the interferon (IFN) system. Our results strongly suggest that lactosylated cationic liposomes have an appropriate mechanism by which to deliver siRNA as a therapy for liver disease.

2. Materials and methods

2.1. siRNAs

The design of HCV-directed siRNA has been described previously [11]. Briefly, we designed nine siRNAs that target the 5′-UTR and 3′-UTR of the HCV genome and examined the efficiency of their inhibition of HCV replication in vitro. Among the nine siRNAs, the most effective siE was used in the present study and was directed toward nucleotides 325–344 of the HCV genome. The target sequence was 5′-GUCUC GUAGACCGUGCAUCAUU-3′. The p53m siRNA (sip53m) [11] and GL3-M1 siRNA (siGL3-M1) were used as the negative controls. The sense sequence of siGL3-M1, which is sequence-specific for firefly luciferase mRNA, was 5′-GCUAUGAAACGAUAUGGGCUU-3′.

2.2. Preparation of cationic liposomes and siRNA/cationic liposome complexes

The cationic liposomes were composed of three lipids: a cationic lipid, phosphatidylcholine (PC), and lactosylated phosphatidylethanolamine (LA-PE). The preparation of the cationic liposomes [24] and the synthesis of the LA-PE [26] have been described previously. The ratio of the two neutral lipids, PC and LA-PE in the liposomes was as follows: CL-LA0, 5:0; CL-LA1, 4:1; CL-LA2, 3:2; CL-LA3, 2:3; CL-LA4, 1:4; and CL-LA5, 0:5. Each siRNA was mixed with 16 times the amount of cationic liposome, resulting in siRNA/CL-LA. The size of every siRNA/CL-LA was controlled as an average 150 nm.

2.3. Inhibition assay of HCV replication in replicon cells

We used two kinds of HCV replicon cells [27]; FLR3-1 (genotype 1b, Con-1; Fig. 1a) [28] and R6FLR-N (genotype 1b, strain N) [11]. siRNA/CL-LA was added to the medium of the HCV replicon cells, FLR3-1 or R6FLR-N, at a final concentration of 30 nM. For positive control [11], HCV replicon cells were transfected with siRNA using Lipofectamine 2000 (Invitrogen, Carlsbad, CA). After 72 h incubation, we performed luciferase assays using the Bright-Glo luciferase assay system (Promega, Madison, WI).

2.4. Immunoblotting

Cells were harvested using lysis buffer [11]. Then 5 μg of protein was separated by 10% SDS–PAGE, and electro-blotted onto a PVDF membrane (Immobilon-P; Millipore, Billerica, MA). Rabbit polyclonal anti-HCV nonstructural protein 3 (NS3) antibody (R212) prepared in our laboratory and mouse monoclonal anti-β-actin antibody (Sigma, St. Louis, MO) were used as the primary antibodies.

2.5. Transfection efficiency of siRNA by CL-LA in vitro

The transfection efficiencies of Cy3-labeled siRNA (Cy3-siRNA) by CL-LA were determined using confocal laser microscopy (Zeiss, Jena, Germany). HCV replicon cells were seeded in the Lab-Tek II Chamber Slide-System (Nalge Nunc International, Rochester, NY) at 2.0×10^4 cells per well. The siRNA was labeled with Cy3 using a Silencer siRNA Labeled Kit (Ambion, Austin, TX). After incubation for 24 h, the cells were fixed in 4% buffered formalin and the nuclei stained using DAPI.

2.6. Animals

Male BALB/c mice at 8 weeks of age were purchased from Japan SLC (Hamamatsu, Japan). BALB/c mice and CN2-29 transgenic mice received human care according to guidelines of the National Institutes of Health. Animal experiment protocols performed in accordance with The Tokyo Metropolitan Institute of Medical Science Animal Experiment Committee.

2.7. siRNA delivery by CL-LA in vivo

Alexa-546 or Alexa-568 labeled siE/CL-LA was intravenously injected into BALB/c mice. After 5 and 30 min, the liver, lung, spleen, and kidney were extirpated from the mouse. Sections of these tissues were then stained with DAPI and slides examined using confocal laser microscopy (Zeiss).
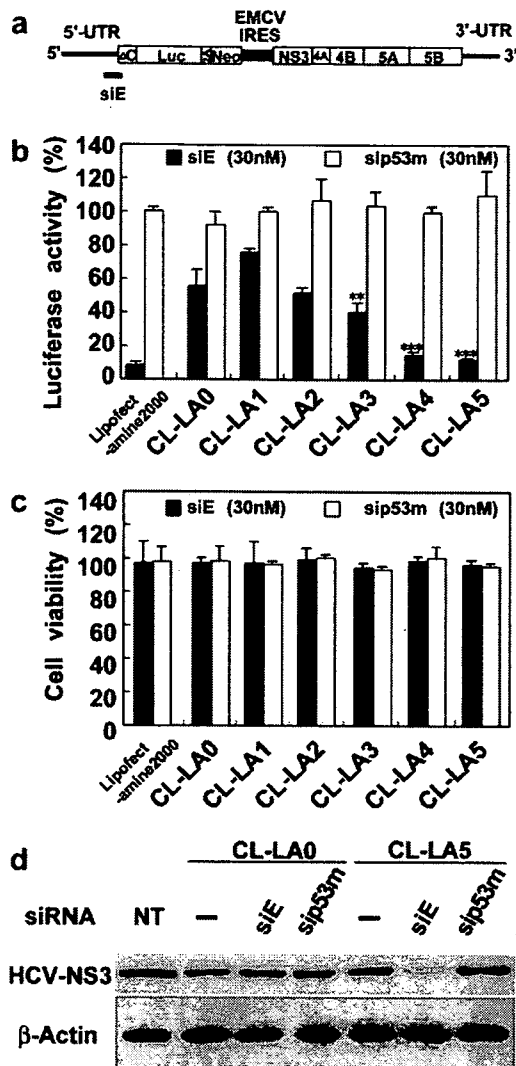
Fig. 1. Effect of siRNA/CL-LA in HCV replicon cells. (a) Schematic representation of HCV replicon RNA and siE position. UTR, untranslated region; ΔC, truncated HCV core region (nucleotides 342–377); Luc, firefly luciferase gene; 2A, 2A genes of foot-and-mouth disease virus; Neo, neomycin resistant gene; EMCV, encephalomyocarditis virus; IRES, internal ribosomal entry site; NS, HCV nonstructural protein; siE, HCV-directed siRNA. (b) FLR3-1 replicon cells were treated with 30 nM siRNA/CL-LA. Luciferase activity was measured after 72 h. Data represent means ± SD compared with mock-transfected cells (n = 5). The average luciferase activities were analyzed by Dennett's test. **P < 0.01 vs. CL-LA0 and ***P < 0.001 vs. CL-LA0. sip53m was used as the negative control. Commercial transfection agent Lipofect-amine 2000 was used as the relative positive control. (c) Cell viability was determined after 72 h. Data represent means ± SD (n = 5) of WST conversion compared with mock-transfected cells. (d) Immunoblot analysis of HCV-NS3 and β-actin. NT, non treatment.

2.8. Gene silencing of HCV genome expression in vivo by siRNA

We used 8- to 10-week-old, 20 g CN2-29 transgenic mice, which contain conditional HCV cDNA, the expression of which is regulated by the Cre/loxP-system (Fig. 4a) [29]. Expression of HCV core protein

is regulated by Cre DNA recombinase in the liver, which can be expressed by administration of adenovirus encoded Cre DNA recombinase (AxCANCre). AxCANCre was intravenously administered at 2×10^9 pfu per body 1 h prior to siRNA (2.5, 5 or 10 mg/kg) injection. After 48 h, expression levels of HCV core protein in the liver were detected using the Ortho HCV core protein ELISA kit (Eiken Chemical, Tokyo, Japan).

2.9. Detection of interferon-β induction by administration of siRNA/CL-LA5 complex

Poly(I):poly(C) was purchased from Yamasa-shoyu (Chiba, Japan). siRNA/CL-LA5 or poly(I):poly(C)/CL-LA5 (200 μg) was intravenously injected into the CN2-29 mice. After 6 h, the livers were extirpated and total RNA was extracted by the acid guanidinium–phenol–chloroform method. cDNA was synthesized from 1 μg of the total RNA using TaqMan reverse transcription reagents (ABI, Foster City, CA). Expression levels of IFN-β mRNA were determined using a Taq-Man gene expression assay kit (ABI) according to the manufacturer's instructions [30,31].

2.10. Statistical analysis

The data are expressed as means ± SD. Statistical analysis was conducted using the analysis of variance with the Dennett's test for multiple comparisons. Statistical significance was established at $P < 0.05$.

3. Results

3.1. Optimization of amount of lactosylated phosphatidylethanolamine (LA-PE) included in the cationic liposomes

To optimize the amount of LA-PE in lactosylated cationic liposomes (CL-LA), we initially prepared six kinds of cationic liposomes containing various amounts of lactose residues, and investigated the inhibitory effects of siE/CL-LA against HCV replication in FLR3-1 replicon cells. The CL-LA strengthened the inhibitory efficiency of siE by increasing the amount of LA-PE. The siE/CL-LA5, which contained LA-PE but not PC, had the strongest inhibitory effect. On the other hand, none of the sip53m/CL-LA affected luciferase activity reflecting the HCV replication (Fig. 1b). To access cytotoxicity of a complex of siRNA and CL-LA, cell viability was measured by the WST-8 assay [11]. None of siE/CL-LA or sip53m/CL-LA showed any cytotoxicity (Fig. 1c). A luciferase assay in another replicon cell line, R6FLR-N replicon [11], showed similar results for HCV-specific silencing (data not shown). Immunoblot analysis showed that the levels of HCV NS3 protein that were translated from the HCV replicon were decreased by siE/CL-LA5, but not by sip53m/CL-LA5 (Fig. 1d). These results indicated that siE/CL-LA5 inhibited HCV replication the most effectively in vitro and that this inhibition was not due to nonspecific reduction caused by the complex of siRNA and CL-LA.

3.2. Transfection efficiency of siRNA by CL-LA5 into HCV replicon cells

To investigate whether lactose residue enhances the transfection of siRNA, we observed fluorescent-labeled siE introduced into RLR3-1 replicon cells. After a 24 h incubation with siE/CL-LA0 or siE/CL-LA5, the cells were observed by fluorescence microscopy (Fig. 2). The lactosylated cationic liposome CL-LA5 transfected siE into replicon cells more effectively than the non-lactosylated cationic liposome CL-LA0. Moreover, fluorescence of siE transfected by CL-LA5 was observed mainly in the cytoplasm, and was more effective than that with the commercial agent Lipofectamine 2000. These results demonstrated that the lactose residue very strongly enhanced the transfection efficiency of siRNA into replicon cells, particularly in the cytoplasm.

3.3. Delivery of siRNA by CL-LA5 in mice

Next, we investigated the delivery of siRNA by CL-LA5 in BALB/c mice, which were intravenously injected with fluorescent-labeled siE/CL-LA0 or siE/CL-LA5 (Fig. 3). At 5 and 30 min after injection via the orbital vein, the livers of the mice were extirpated and observed by fluorescence microscopy. The fluorescence intensity of siE/CL-LA5 at 5 min was clearly stronger than that of siE/CL-LA0. At 30 min after injection, fluorescence of siE/CL-LA5 was equally spread throughout the hepatic parenchymal cells, although that of siE/CL-LA0 could be patchily detected in parts (Fig. 3a). These results demonstrated that CL-LA5 could more easily take siRNA into the cytoplasm of parenchymal liver cells. Furthermore, we also examined the tissue distribution of siRNA delivered by CL-LA5 (Fig. 3b). At

30 min after injection, the liver, spleen, kidney and lung of another mouse were excised and the intensity of fluorescence of labeled-siE in these tissues calculated. Although the relative fluorescence of siE/CL-LA0 accumulated in the liver and spleen, that of siE/CL-LA5 accumulated primarily in the liver alone, and the residual fluorescence of siE was equally diffused in other tissues. Taken together, these results indicated that CL-LA5 was able to trap siRNA primarily in the mouse liver, where it could be efficiently taken up into the hepatocytes.

3.4. Down-regulation of HCV protein expression by siE/CL-LA5 in transgenic mouse liver

To extend our findings of the in vitro silencing effect by siE/CL-LA5 and in vivo siRNA delivery by CL-LA5, we performed an additional study in an HCV transgenic mouse model [29]. We administered siE/CL-LA5 to CN2-29 mice after inducing HCV protein expression by AxCANCre (Fig. 4b). The mice were sacrificed on the second day after injection, and expression of HCV core protein in the liver measured by ELISA. The siE/CL-LA5 decreased the amount of core protein in a dose-dependent manner. The maximal dose of HCV unrelated siGL3-M1/CL-LA5 did not inhibit the expression of HCV core protein. These results demonstrated that siE/CL-LA5 specifically inhibited HCV protein expression in mouse liver.

3.5. IFN response by siRNA/CL-LA5 in vivo

It has been reported that siRNA can activate the cellular interferon (IFN) pathway, especially when delivered by cationic liposome transfection reagents [32,33].
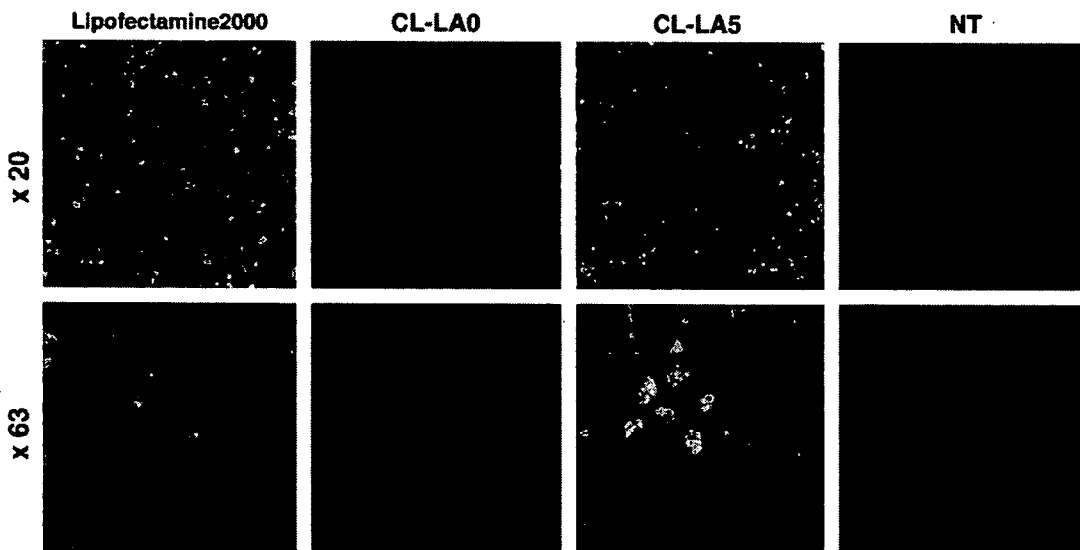

Fig. 2. Transfection efficiency of fluorescent-labeled siRNA into HCV replicon cells. FLR3-1 replicon cells were treated with CL-LA0, CL-LA5, or Lipofectamine 2000 complexed with Cy3-labeled siE (100 nM). After incubation for 48 h, the cells were observed by fluorescence microscopy. The nuclei were stained with DAPI. NT, non treatment.